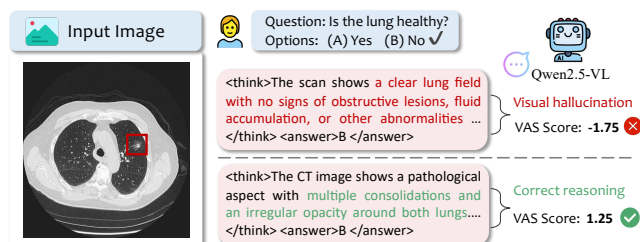


# Learn to Think: Improving Multimodal Reasoning through Vision-Aware Self-Improvement Training

Qihuang Zhong<sup>1</sup> Liang Ding<sup>2</sup> Wenjie Xuan<sup>1</sup> Juhua Liu<sup>1</sup> Bo Du<sup>1</sup> Dacheng Tao<sup>3</sup>

## Abstract

Post-training with explicit reasoning traces is common to improve the reasoning capabilities of Multimodal Large Language Models (MLLMs). However, acquiring high-quality reasoning traces is often costly and time-consuming. Hence, the *self-improvement* paradigm has emerged, enabling MLLMs to self-generate reasoning traces for training without external supervision. Despite its effectiveness, we reveal two shortcomings in the self-improvement training of MLLMs: 1) data imbalance, where simple samples are over-trained, but the challenging yet crucial samples are under-trained; 2) language prior bias, where MLLMs overly rely on linguistic priors while neglecting the visual cues. To this end, we propose **VISTA**, a **V**ision-aware **S**elf-improvement **T**raining framework for enhancing the multimodal reAsoning of MLLMs. Specifically, VISTA first introduces a *prefix resampling* strategy to reuse the partial correct reasoning traces for efficient data collection, and then designs a *vision-aware attention score* to quantify the model’s focus on visual information. Extensive experiments show that VISTA can be applied to various post-training scenarios, *i.e.*, supervised fine-tuning and preference learning, and effectively enhances the multimodal reasoning performance across various MLLMs and tasks, *e.g.*, bringing up to **+13.66%** average performance gains for Qwen2.5-VL-3B-Instruct.



**Figure 1. Comparison of two self-generated reasoning traces.** As seen, although predicting the correct answer, MLLMs may still exhibit visual hallucinations during intermediate reasoning processes, due to over-reliance on language priors and neglect of visual cues. Encouragingly, our proposed vision-aware attention score (VAS) can accurately identify these hallucinated solutions.

## 1. Introduction

Inspired by the success of OpenAI o1/o3 (Jaech et al., 2024) and DeepSeek-R1 (Guo et al., 2025), multimodal reasoning, which extends long chain-of-thought (CoT) capabilities to multimodal large language models (MLLMs), has recently attracted significant research attention (Wang et al., 2024b; 2025). While post-training with explicit reasoning trajectories can effectively enhance the multimodal reasoning of MLLMs, their performance highly relies on high-quality intermediate reasoning traces (Yang et al., 2025b), which are expensive and time-consuming to obtain (Peng et al., 2025). Hence, recent literature (Deng et al., 2025) introduces a *self-improvement* paradigm, where MLLMs iteratively improve themselves by training with their self-generated reasoning data, thus reducing the reliance on external supervision.

In general, self-improvement training usually contains three steps: (1) data collection, where models are prompted to generate multiple reasoning solutions for each query; (2) data organization, where the ground-truth answers are used to verify the correctness of candidate solutions and the incorrect solutions will be filtered out; (3) model optimization, where models are self-trained with the selected correct solutions. Although self-improvement training has demonstrated remarkable performance (Zelikman et al., 2022; Singh et al., 2023), through a series of analyses (§2.1), we reveal that the self-improvement of MLLMs still suffers from two key shortcomings: ❶ *data imbalance*, *i.e.*, during data collec-

<sup>1</sup>School of Computer Science, National Engineering Research Center for Multimedia Software, Institute of Artificial Intelligence and Hubei Key Laboratory of Multimedia and Network Communication Engineering, Wuhan University, China <sup>2</sup>The University of Sydney, Australia <sup>3</sup>Nanyang Technological University, Singapore. Correspondence to: Juhua Liu <liujuhua@whu.edu.cn>.

Proceedings of the 43<sup>rd</sup> International Conference on Machine Learning, Seoul, South Korea. PMLR 306, 2026. Copyright 2026 by the author(s).

tion, MLLMs can readily generate numerous correct solutions for simple queries but struggle to produce sufficient correct ones for difficult queries; ② *language prior bias*, *i.e.*, MLLMs tend to over-rely on language priors while neglecting visual cues, leading to visual hallucinations that cannot be filtered by answer correctness alone (as illustrated in Figure 1). Notably, these two problems share a common root: current self-improvement methods rely solely on answer correctness as the quality signal. This single signal proves inadequate in two complementary ways: (1) in *quantity*, it fails to yield sufficient correct solutions for challenging queries; (2) in *quality*, it cannot distinguish visually-grounded solutions from hallucinated ones that happen to arrive at correct answers. These observations naturally give rise to two questions: 1) *How can we obtain sufficient correct solutions for challenging yet crucial queries?* 2) *How can we effectively identify and filter out undesired hallucinated solutions?*

Some prior studies also recognize these issues and attempt to address them (Tong et al., 2024; Ding et al., 2025; He et al., 2025). For ①, Tong et al. (2024) propose to allocate more trials to difficult queries, and Ding et al. (2025) attempt to use the ground-truth answers to guide the reasoning. Although effective, these methods neglect the prior failed solutions that also contain some useful information, which are wasted and inefficient. For ②, He et al. (2025) design a metric to quantify the language prior bias by removing the image context and measuring the change of attention scores. Despite its remarkable performance, it requires two forward passes, leading to much computation overhead.

Different from prior works, in this paper, we propose **VISTA**, a **V**ision-aware **S**elf-improvement **T**raining framework that enhances the multimodal re**A**soning of MLLMs via two novel strategies. First, to alleviate data imbalance, inspired by prior findings (Ji et al., 2025) – *errors of failed solutions often occur in the later reasoning traces*, we introduce a **prefix resampling** strategy that reuses the correct prefix contexts from failed solutions for efficient data collection. In practice, it first identifies partially correct reasoning traces by locating the critical tokens that exert a significant influence on subsequent reasoning steps, and then uses these traces as prefix context to resample new solutions. Second, to mitigate the language prior bias, we design a simple-yet-effective **Vision-aware Attention Score** (VAS) approach that leverages the model’s internal attention information to quantify its focus on the visual cues during reasoning. Intuitively, if the model allocates limited attention to the visual context, it may drift away from the visual cues, thus leading to potential visual hallucinations. Overall, by collecting more correct solutions for difficult queries and filtering the undesired solutions with lower VAS, VISTA can ensure the diversity and reliability of self-training data, thus bringing better reasoning performance for MLLMs.

Extensive experiments on five cutting-edge MLLMs and five popular multimodal reasoning tasks show that VISTA not only outperforms all counterparts by a clear margin, *i.e.*, bringing up to **+13.66%** average performance gains against the initial reasoning models, but also works well in various post-training paradigms, *e.g.*, supervised fine-tuning and preference learning. More encouragingly, in-depth analyses prove that VISTA reduces the visual hallucinations and improves the out-of-distribution (OOD) performance effectively. To summarize, our contributions are three-fold: (1) We reveal two shortcomings of self-improvement training in MLLMs, and propose VISTA to address them and boost MLLMs’ multimodal reasoning capabilities without extra supervision. (2) VISTA introduces two simple-yet-effective strategies that can be adopted to various MLLMs and post-training settings. (3) Extensive results show that VISTA can significantly and consistently improve MLLMs’ multimodal reasoning performance and model generalization.

## 2. Revisiting Self-improvement in MLLMs

### 2.1. Preliminary

Given a base MLLM  $\mathcal{M}_{base}$  and a multimodal dataset  $\mathcal{D} = \{(x_i, y_i)\}$ , where  $x_i = \{x_i^{sys}, x_i^{vis}, x_i^{ins}\}$  is the query and  $y_i$  is corresponding ground-truth answer.  $x_i^{sys}$ ,  $x_i^{vis}$ ,  $x_i^{ins}$  denote the system prompt, visual, and user instruction tokens, respectively. The goal of self-improvement training is to enhance the long-CoT multimodal reasoning performance of  $\mathcal{M}_{base}$  by iteratively self-training using its own solutions on  $\mathcal{D}$  over  $T$  cycles. Let  $\mathcal{M}_t$  denote the model at the  $t$ -th iteration ( $t \in [1, T]$ ). The representative self-improvement training for MLLMs involves the following steps:

**Data Collection.** At  $t$ -th iteration, for each query  $x_i \in \mathcal{D}$ , we enforce the previous  $\mathcal{M}_{t-1}$  to generate multiple reasoning trajectories and their corresponding answers  $\{(r_i^k, \hat{y}_i^k)\}_{k=1}^K$ , where  $K$  denotes the sampling time for each query and  $r_i^k$  denotes the  $k$ -th trajectory. Thus, we can construct the self-generated dataset  $\mathcal{D}_t = \{(x_i, r_i^k, \hat{y}_i^k)_{k=1}^K\}$ .

**Data Organization.** The ground-truth answer  $y_i$  is used to verify the correctness of candidate solutions. According to the correctness, we can split the candidate solutions into two sets: positive set  $\mathcal{D}_t^p = \{(x_i, r_i^{k_p}, \hat{y}_i^{k_p}) \mid \mathbb{I}(\hat{y}_i^{k_p}, y_i) = 1\}$  and negative set  $\mathcal{D}_t^n = \{(x_i, r_i^{k_n}, \hat{y}_i^{k_n}) \mid \mathbb{I}(\hat{y}_i^{k_n}, y_i) = 0\}$ .

**Model Optimization.** The self-training process differs across various post-training paradigms, *i.e.*, supervised fine-tuning (SFT) and preference learning. Specifically, for self-improvement SFT training, only the correct solutions from  $\mathcal{D}_t^p$  are used to optimize the model via the standard negative log likelihood (NLL) loss function:

$$\mathcal{L}_{\text{SFT}} = \mathbb{E}_{\mathcal{D}_t^p} \left[ -\log \frac{\mathcal{M}_\theta(r_i^{k_p}, \hat{y}_i^{k_p} | x_i)}{|r_i^{k_p}| + |\hat{y}_i^{k_p}|} \right], \quad (1)$$

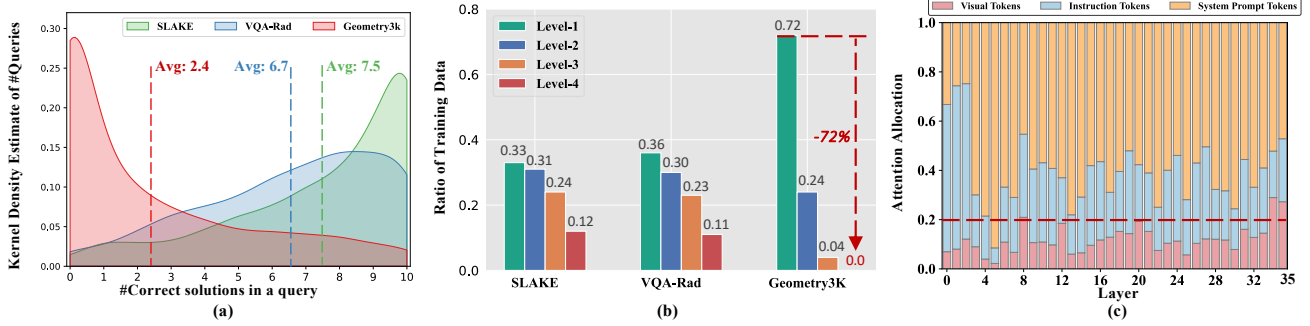


Figure 2. (a) Distribution of the number of correct solutions in a single query. (b) Distribution of self-generated training samples for different difficulty levels, where level-1 denotes the simplest and level-4 denotes the hardest. (c) Attention allocation between system prompts, visual, and instruction tokens across different model layers. Here, we use the Qwen2.5-VL-3B-Instruct as the base model.

where  $\mathcal{M}_\theta$  initialized with  $\mathcal{M}_{base}$  denotes the current tuned model that will become next model  $\mathcal{M}_t$ . Notably, following previous practice (Zelikman et al., 2022; Singh et al., 2023), we do not continually fine-tune  $\mathcal{M}_{t-1}$  to avoid overfitting.

For the implementation of preference learning, we use the representative Direct Preference Optimization (DPO) (Rafailov et al., 2023). In practice, each positive solution in  $\mathcal{D}_t^p$  and a randomly-selected negative solution from  $\mathcal{D}_t^n$  are paired to construct the preference training set  $\mathcal{D}_t^{pairs} = \{(x_i, r_i^{k_p}, \hat{y}_i^{k_p}, r_i^{k_n}, \hat{y}_i^{k_n}) \mid k_p, k_n \in [1, K]\}$ . Then, inspired by Pang et al. (2024), we leverage an enhanced DPO algorithm that combines the standard DPO and NLL loss functions to ensure the training stability:

$$\begin{aligned} \mathcal{L}_{DPO+NLL} &= \mathcal{L}_{DPO} + \alpha \cdot \mathcal{L}_{NLL}(r_i^{k_p}, \hat{y}_i^{k_p}) \\ &= \mathbb{E}_{\mathcal{D}_t^{pairs}} \left[ -\log \sigma \left( f(\hat{r}_i^{k_p}, \hat{y}_i^{k_p} | x_i) - f(\hat{r}_i^{k_n}, \hat{y}_i^{k_n} | x_i) \right) \right. \\ &\quad \left. - \alpha \cdot \frac{\log \mathcal{M}_\theta(\hat{r}_i^{k_p}, \hat{y}_i^{k_p} | x_i)}{|\hat{r}_i^{k_p}| + |\hat{y}_i^{k_p}|} \right], \end{aligned} \quad (2)$$

where  $f(\cdot | x_i) = \beta \log \frac{\mathcal{M}_\theta(\cdot | x_i)}{\mathcal{M}_{base}(\cdot | x_i)}$ ,  $\mathcal{M}_\theta$  is the policy model initialized with  $\mathcal{M}_{base}$ ,  $\sigma$  is the sigmoid function.  $\alpha$  and  $\beta$  are coefficients that are empirically set to 0.5 and 0.1. Notably, to ensure the initial model has basic reasoning capabilities, we use some reasoning examples as few-shot demonstrations to prompt  $\mathcal{M}_{base}$  to sample multiple reasoning solutions for each query. By randomly selecting one correct solution per query, we construct a seed training set and use it to fine-tune  $\mathcal{M}_{base}$  for obtaining the initial  $\mathcal{M}_0$ .

## 2.2. Empirical Analyses

**Settings.** Here, we use the Qwen2.5-VL-3B-Instruct (Bai et al., 2025b) model and several popular multimodal reasoning benchmarks, *i.e.*, SLAKE (Liu et al., 2021), VQA-Rad (Lau et al., 2018) and Geometry3K (Lu et al., 2021), as a testbed. During the implementation of self-improvement training, the sampling time  $K$  is set to 10, and the number of iterations  $T$  is set to 1 for faster experimental validation.

**Findings.** Through a series of analyses on the self-generated samples, we empirically found two issues:

① **Data Imbalance:** First, we illustrate the distribution of the number of self-generated correct solutions per query in Figure 2 (a). As seen, the number of correct solutions is highly related to task difficulty, where MLLMs can produce numerous correct solutions for simpler tasks (*i.e.*, SLAKE) but struggle to generate sufficient correct ones for harder tasks (*i.e.*, Geometry3K). Specifically, for Geometry3K, there are more than 40% queries without any correct solutions. Unfortunately, these challenging queries are proven to be more crucial for further training (Liu et al., 2024). To have a closer look, we evenly split all queries into four levels based on the number of correct solutions per query, and illustrate the distribution of self-generated training samples at different levels in Figure 2 (b). Obviously, most self-generated samples are simple, whereas the challenging yet crucial samples are scarce, especially in harder tasks.

② **Language Prior Bias:** By analyzing the candidate solutions in  $\mathcal{D}_t^p$ , we found that, while some solutions make the correct predictions, they may exhibit hallucination issues in the reasoning traces, *e.g.*, describing some things that do not exist in the image, or exhibiting a conflict between the reasoning chain and its final answer. Some examples are provided in Figure 9 of Appendix C.2. To investigate this problem, inspired by prior works (Leng et al., 2024; Liu et al., 2025a; He et al., 2025) related to hallucination alleviation, we leverage the model’s internal attention information to directly probe the model’s behavior. Specifically, we follow Liu et al. (2025a) and compare the attention distributions of the first output token over visual, instruction, and system prompt tokens across all layers. In practice, we randomly sample 100 data points from the training set of VQA-Rad, and illustrate the average attention distributions in Figure 2 (c). It can be found that, although visual tokens account for the largest proportion in the context, they generally receive the lowest attention scores (less than 20% in most layers) across all layers. Conversely, the model tends

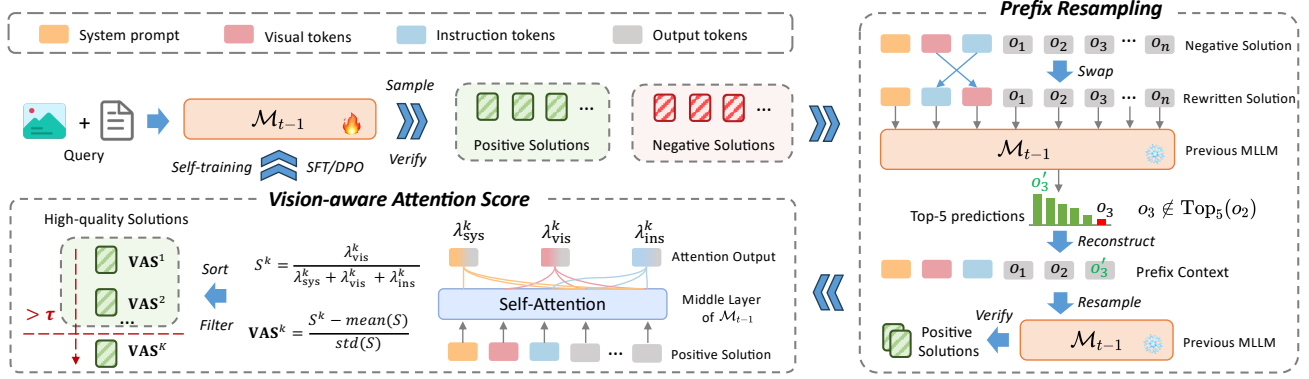


Figure 3. Overview of our VISTA framework, which consists of two simple-yet-effective strategies: 1) *prefix resampling*, aiming to collect more accurate solutions for difficult queries; 2) *vision-aware attention score*, aiming to filter out undesired hallucinated solutions.

to focus on the linguistic information of instruction and system prompt tokens. We conjecture that visual hallucinations in MLLMs may originate from such a language prior bias.

### 3. Methodology

**Motivation of VISTA.** To address the above problems, we propose VISTA that harnesses self-improvement in MLLMs via two simple-yet-effective approaches. First, for ❶, we build upon the insight (Ji et al., 2025; Yang et al., 2025a) that *errors of failed solutions often occur in the later reasoning traces, while early reasoning steps are usually correct and informative*. Instead of discarding these valuable prior failed solutions, we introduce *prefix resampling* to accurately locate the partially correct prefix and reuse it to achieve efficient data collection. Second, for ❷, motivated by the empirical analysis in §2.2, we recognize that the internal information of MLLMs’ attention heads can reflect the language prior bias effectively. Hence, we further introduce *Vision-aware Attention Score* (VAS), an efficient metric that measures the attention allocation over visual tokens in reasoning trajectories to quantify the model’s focus on visual cues. Figure 3 illustrates the overview of VISTA, and the pseudo-code of VISTA is shown in Algorithm 1.

**Prefix Resampling.** The core of prefix resampling is to locate the correct prefix. Motivated by the concept of *critical tokens* – some output tokens exert significant influence on later reasoning steps (Lin et al., 2025), we attempt to make full use of MLLMs’ self-calibration abilities to locate these critical tokens from prior solutions without relying on ground-truth answers and extra models. Specifically, for each sample in  $\mathcal{D}_t^n$ , we construct a new query by swapping the position<sup>1</sup> of the image, *e.g.*, from “ $x_i^{\text{vis}} + x_i^{\text{ins}}$ ” to “ $x_i^{\text{ins}} + x_i^{\text{vis}}$ ”, and concatenate the new query with prior reasoning traces, *i.e.*, “ $x_i^{\text{sys}} + x_i^{\text{ins}} + x_i^{\text{vis}} + r_i^{k_n}$ ”. The recon-

<sup>1</sup>The effectiveness of the swap method, along with further empirical analysis, is provided in Appendix C.1.

structed sample is fed into  $\mathcal{M}_{t-1}$  to obtain the Top-5 token predictions<sup>2</sup> at the next position for each reasoning token, denoted as  $\text{Top}_5(o_n)$ , where  $o_n$  means the  $n$ -th token in the reasoning trajectory. The first token that does not match the expected Top-5 tokens, *i.e.*,  $o_n \notin \text{Top}_5(o_{n-1})$ , is regarded as the critical token. Then, we replace the  $o_n$  with the new Top-1 predicted token  $o'_n = \text{Top}_1(o_{n-1})$  and truncate the subsequent reasoning steps. Lastly, we concatenate the original query with truncated reasoning traces as a prefix and resample the subsequent reasoning steps for  $J$  times to collect the correct solutions, which are merged into  $\mathcal{D}_t^p$ .

**Vision-aware Attention Score.** To alleviate the language prior bias, we leverage the MLLMs’ internal attention information to quantify the model’s focus on visual cues. Specifically, for each correct solution  $(x_i^{\text{sys}}, x_i^{\text{vis}}, x_i^{\text{ins}}, r_i^k, \hat{y}_i^k)$  in  $\mathcal{D}_t^p$ , we extract its attention output  $\mathbf{A}_i^k$  from an intermediate layer of  $\mathcal{M}_{t-1}$ . Since the middle layers play a crucial role in processing visual information (Jiang et al., 2025), we select the middle layer of  $\mathcal{M}_{t-1}$  in this work (further analyses are provided in Appendix C.2). Then, we measure the attention allocation assigned by the output reasoning tokens to different contexts:

$$\begin{aligned} \lambda_{\text{sys}}^k &= \sum_o (r_i^k, \hat{y}_i^k) \sum_{x_i^{\text{sys}}} \mathbf{A}_i^k(o, s), \\ \lambda_{\text{vis}}^k &= \sum_o (r_i^k, \hat{y}_i^k) \sum_{x_i^{\text{vis}}} \mathbf{A}_i^k(o, s), \\ \lambda_{\text{ins}}^k &= \sum_o (r_i^k, \hat{y}_i^k) \sum_{x_i^{\text{ins}}} \mathbf{A}_i^k(o, s), \end{aligned} \quad (3)$$

where  $\lambda_{\text{sys}}^k$ ,  $\lambda_{\text{vis}}^k$ , and  $\lambda_{\text{ins}}^k$  denote the attention allocation over system tokens, visual tokens, and instruction tokens, respectively. Based on it, we leverage the degree of  $\lambda_{\text{vis}}^k$  to quantify the focus of MLLMs on visual cues, and regularize different scores using a standard normalization:

$$S_i^k = \frac{\lambda_{\text{vis}}^k}{\lambda_{\text{sys}}^k + \lambda_{\text{vis}}^k + \lambda_{\text{ins}}^k}, \text{VAS}_i^k = \frac{S_i^k - \text{mean}(S_i)}{\text{std}(S_i)}, \quad (4)$$

<sup>2</sup>The effect of the Top- $k$  setting is analyzed in Appendix C.1.

where  $\text{VAS}_i^k$  refers to our proposed VAS score. The undesired solutions with scores below the threshold  $\tau$  are filtered, and the remaining high-quality correct solutions are used to perform the iterative self-improvement training.

Intuitively, by paraphrasing the query and verifying whether the prior generated token matches the expected token predictions, we can leverage MLLMs’ self-calibration capabilities to identify uncertain tokens that may lead to deviating from the correct reasoning trajectory. Moreover, by replacing these uncertain tokens with more reliable ones, we can efficiently resample more accurate solutions for difficult queries. Furthermore, we use our VAS metric to filter out the undesired solutions that overly rely on language priors. By doing so, VISTA can construct a more diverse and reliable reasoning dataset, thus leading to better performance.

## 4. Experiments

### 4.1. Experimental Setup

**Tasks and Datasets.** We mainly assess the effectiveness of VISTA on multimodal medical reasoning and mathematical reasoning tasks, *i.e.*, using the SLAKE (Liu et al., 2021) and VQA-Rad (Lau et al., 2018) for medical reasoning, while using the Geometry3K (Lu et al., 2021) (Geo3K for short) for mathematical reasoning. Moreover, to verify the universality of VISTA, we also evaluate on two popular multimodal reasoning benchmarks, including the ScienceQA (Lu et al., 2022) and ChartQA (Masry et al., 2022). For each task, we post-train MLLMs on the training set and evaluate them on the corresponding test set by using the zero-shot accuracy as the metric. Following DeepSeek-R1 (Guo et al., 2025), the reasoning process and answer are enclosed with `<think></think>` and `<answer></answer>`. More details of the used datasets are shown in Appendix B.1.

**Training Details.** We conduct main experiments using several cutting-edge and powerful MLLMs, including Qwen2.5-VL-3B/7B-Instruct (Bai et al., 2025b), Qwen3-VL-2B-Instruct (Bai et al., 2025a), InternVL3-2B/8B (Zhu et al., 2025) models. During the implementation of our VISTA, the sampling times  $K$  and  $J$  are set to 10 and 3, respectively. The sampling temperature is 1.0, and the maximum output length is 2,048. The threshold  $\tau$  is set to -0.5. For the SFT of Qwen2.5-VL models, we set the self-improvement iteration  $T$  to 3. Notably, due to the limited computational resources, for the other models, we only perform the self-improvement training for one iteration, *i.e.*,  $T = 1$ . During model inference, greedy decoding with a maximum output length of 2,048 is used for reproducibility. All models are post-trained for 3 epochs on 8 NVIDIA A800 (80GB) GPUs. More training and inference details are provided in Appendix B.2.

**Baselines.** We compare VISTA with several representa-

tive and cutting-edge self-improvement training methods:

- **SFT-Seed:** Standard fine-tuning  $\mathcal{M}_{base}$  on the self-generated seed data  $\mathcal{S}$  to obtain the initial model  $\mathcal{M}_0$ .
- **SFT-Oracle:** Standard fine-tuning  $\mathcal{M}_{base}$  on  $\mathcal{D}$  with reasoning trajectories distilled from a third-party MLLM, *i.e.*, Qwen3-VL-32B-Instruct, which can be considered as the upper bound of self-improvement SFT training.
- **STaR** (Zelikman et al., 2022): Sampling a solution using greedy decoding for each query in  $\mathcal{D}$ , where the correct solutions are used to iteratively fine-tune  $\mathcal{M}_{base}$ .
- **ReST<sup>EM</sup>** (Singh et al., 2023): Extending STaR by sampling  $K$  solutions for each query in  $\mathcal{D}$ , where all correct solutions are used for iterative SFT training.
- **RFT** (Yuan et al., 2023): Similar to ReST<sup>EM</sup> but not iterative. To maintain consistent training budgets, we sample  $T \times K$  candidate solutions for each query in  $\mathcal{D}$ .
- **R3V** (Cheng et al., 2025): Extending ReST<sup>EM</sup> by additionally using the incorrect solutions to construct self-refine and self-select data for iterative SFT training.
- **IRPO** (Pang et al., 2024): Sampling  $K$  solutions for each query, where correct and incorrect solutions are paired to construct the preference data for iterative DPO training.

For a fair comparison, we keep a fixed data synthesis budget for all baselines, except STaR. Considering our goal of proposing a self-improvement training method, in this part, we do not compare VISTA with inference-time methods, *e.g.*, self-consistency (Wang et al., 2023). More comparisons with inference-time methods are shown in Appendix C.3.

### 4.2. Main Results

**VISTA outperforms the other baseline methods by a clear margin.** Table 1 reports the comparative results (%) of Qwen2.5-VL family models on medical and mathematical reasoning tasks. As seen, compared to the SFT-Seed baseline, almost all self-improvement methods bring some performance improvements, proving the effectiveness of the self-improvement training paradigm. Among which, our VISTA outperforms all counterparts and leads to the highest performance gains, *i.e.*, **+13.66%** and **+6.67%** average scores for 3B and 7B Qwen2.5-VL models, respectively. It is noteworthy that some baseline methods suffer from model collapse, where the model’s performance degrades due to iterative self-training on model-generated data (Bertrand et al., 2024), especially in the harder Geometry3K task. We attribute it to the data imbalance problem, as over-training on the simple queries could lead to over-fitting. Conversely, by sampling more accurate solutions for challenging queries,

**Learn to Think: Improving Multimodal Reasoning through Vision-Aware Self-Improvement Training**

*Table 1. Performance comparison between Qwen2.5-VL family models using different training methods on medical and mathematical multimodal reasoning benchmarks. “|Train|” means the average number of training samples among all models and tasks. “Overall” denotes the average accuracy, while the subscript results denote the performance gains against the SFT-Seed. Best results are in **bold**.*

Methods	Train  Avg.	Qwen2.5-VL-3B-Instruct				Qwen2.5-VL-7B-Instruct			
		SLAKE	VQA-Rad	Geo3K	Overall ( $\Delta$ )	SLAKE	VQA-Rad	Geo3K	Overall ( $\Delta$ )
SFT-Seed	1.0K	67.04	64.14	25.46	52.21	79.15	70.52	36.94	62.20
SFT-Oracle	1.3K	81.97	68.13	37.94	62.68 <sub>↑10.47</sub>	82.25	70.12	41.43	64.60 <sub>↑2.40</sub>
RFT	25.5K	79.15	70.12	28.79	59.35 <sub>↑7.14</sub>	82.82	74.90	40.27	66.00 <sub>↑3.80</sub>
STaR									
Iteration 1	0.9K	73.80	66.13	32.11	57.35 <sub>↑5.14</sub>	80.00	71.31	37.44	62.92 <sub>↑0.72</sub>
Iteration 2	1.0K	76.90	65.34	31.95	58.06 <sub>↑5.85</sub>	80.00	72.11	37.94	63.35 <sub>↑1.15</sub>
Iteration 3	1.1K	80.28	69.32	30.78	60.13 <sub>↑7.92</sub>	84.23	69.72	37.10	63.68 <sub>↑1.48</sub>
ReST <sup>EM</sup>									
Iteration 1	8.5K	76.06	69.72	29.95	58.58 <sub>↑6.37</sub>	82.82	73.31	35.77	63.97 <sub>↑1.77</sub>
Iteration 2	9.9K	79.38	71.31	31.45	60.71 <sub>↑8.50</sub>	84.79	74.49	39.77	66.35 <sub>↑4.15</sub>
Iteration 3	10.7K	81.69	73.71	32.28	62.56 <sub>↑10.35</sub>	84.51	75.30	38.94	66.25 <sub>↑4.05</sub>
R3V									
Iteration 1	18.5K	78.21	65.74	29.62	57.89 <sub>↑5.68</sub>	82.82	75.30	36.44	64.85 <sub>↑2.65</sub>
Iteration 2	18.8K	82.82	74.10	32.61	63.18 <sub>↑10.97</sub>	86.48	75.30	38.44	66.74 <sub>↑4.54</sub>
Iteration 3	18.7K	81.41	69.32	32.78	61.17 <sub>↑8.96</sub>	87.32	75.70	37.27	66.76 <sub>↑4.56</sub>
<b>VISTA-SFT (Ours)</b>									
Iteration 1	7.7K	80.85	74.10	32.28	62.41 <sub>↑10.20</sub>	83.66	74.90	40.77	66.44 <sub>↑4.24</sub>
Iteration 2	8.1K	83.38	72.51	34.28	63.39 <sub>↑11.18</sub>	84.79	75.30	41.26	67.12 <sub>↑4.92</sub>
Iteration 3	8.3K	<b>84.23</b>	<b>76.10</b>	<b>37.27</b>	<b>65.87</b> <sub>↑13.66</sub>	<b>87.89</b>	<b>77.29</b>	<b>41.43</b>	<b>68.87</b> <sub>↑6.67</sub>

*Table 2. Performance comparison on more MLLMs tuned with different self-improvement SFT methods on several reasoning benchmarks. In this experiment, we perform the self-improvement training for one iteration. Best results are in **bold**.*

Methods	Qwen3-VL-2B-Instruct			InternVL3-2B			InternVL3-8B			Overall ( $\Delta$ )
	SLAKE	VQA-Rad	Geo3K	SLAKE	VQA-Rad	Geo3K	SLAKE	VQA-Rad	Geo3K	
SFT-Seed	69.86	68.92	32.61	71.54	58.96	26.12	84.51	75.70	41.60	58.87
SFT-Oracle	80.28	68.92	37.43	81.97	72.11	32.78	86.10	76.49	45.59	64.63 <sub>↑5.76</sub>
STaR	75.21	65.34	34.28	71.55	66.53	29.78	85.92	74.50	41.93	60.56 <sub>↑1.69</sub>
STaR+	78.87	69.32	33.78	81.41	68.92	31.28	86.76	72.51	43.43	62.92 <sub>↑4.05</sub>
R3V	81.69	66.14	35.77	80.00	72.31	29.12	87.04	72.51	43.76	63.15 <sub>↑4.28</sub>
<b>VISTA-SFT</b>	<b>81.97</b>	<b>71.31</b>	<b>36.27</b>	<b>82.54</b>	<b>72.51</b>	<b>31.45</b>	<b>87.61</b>	<b>78.49</b>	<b>45.59</b>	<b>65.30</b> <sub>↑6.43</sub>

our VISTA can alleviate this problem and continue to bring better performance gains, proving its effectiveness.

**VISTA brings consistent and significant performance gains across various models and tasks.** In addition to evaluating Qwen2.5-VL models on medical and mathematical tasks, we also adopt our VISTA method to more models and tasks. Specifically, Table 2 reports the comparative results on the other MLLMs, and Table 3 presents the results of different tuned Qwen2.5-VL models on more tasks. Notably, in both experiments, we only perform the self-improvement SFT training for one iteration. On the one hand, from Table 2, we see that our VISTA still works in all these models, and achieves the best performance (even outperforms the SFT-Oracle) among all settings. Specifically, compared to SFT-Seed, VISTA brings **+6.43%** average performance gains. On the other hand, as shown in Table 3, our VISTA consistently outperforms the other counterparts

by a clear margin in both ScienceQA and ChartQA tasks. These results can prove the generality of VISTA.

**VISTA can be applied to various post-training paradigms.** In the above experiments, we evaluate our VISTA in the self-improvement SFT training setting. Here, we conduct more experiments to verify whether VISTA works well in the other post-training paradigms, *i.e.*, DPO (Rafailov et al., 2023) and GRPO (Shao et al., 2024) training. For DPO training, we compare VISTA with the IRPO (Pang et al., 2024) baseline, both of which aim to optimize the base model  $\mathcal{M}_{base}$  with the self-generated preference data. As for GRPO training, we initialize the policy model with the cold-start models tuned with different methods. The ReST<sup>EM</sup> is used as the baseline in this setting. In both experiments, we use the Qwen2.5-VL-3B-Instruct as the base model and perform the self-improvement post-training for one iteration. The comparative results are shown

Table 3. Performance comparison between different tuned Qwen2.5-VL models on **more reasoning benchmarks**.

Methods	Qwen2.5-VL-3B		Qwen2.5-VL-7B	
	ScienceQA	ChartQA	ScienceQA	ChartQA
SFT-Seed	74.66	60.82	81.55	72.32
SFT-Oracle	82.00	65.98	85.49	75.34
STaR	77.49	61.18	84.39	72.46
STaR+	78.60	61.89	85.73	72.81
R3V	80.81	61.31	86.83	73.10
<b>VISTA-SFT</b>	<b>82.29</b>	<b>62.09</b>	<b>87.58</b>	<b>73.68</b>

Table 4. Performance comparison between tuned Qwen2.5-VL-3B-Instruct models using **different post-training algorithms**.

Methods	SLAKE	VQA-Rad	Geo3K	Overall ( $\Delta$ )
SFT-Seed	67.04	64.14	25.46	52.21
<i>(a) DPO Training</i>				
IRPO	86.20	74.10	29.11	63.14 $\uparrow$ 10.93
<b>VISTA-DPO</b>	<b>89.01</b>	<b>76.89</b>	<b>29.45</b>	<b>65.12</b> $\uparrow$ 12.91
<i>(b) GRPO Training, initialized by SFT models</i>				
ReST <sup>EM</sup> -GRPO	84.51	78.09	32.45	65.02 $\uparrow$ 12.81
<b>VISTA-GRPO</b>	<b>85.35</b>	<b>79.28</b>	<b>32.61</b>	<b>65.75</b> $\uparrow$ 13.54

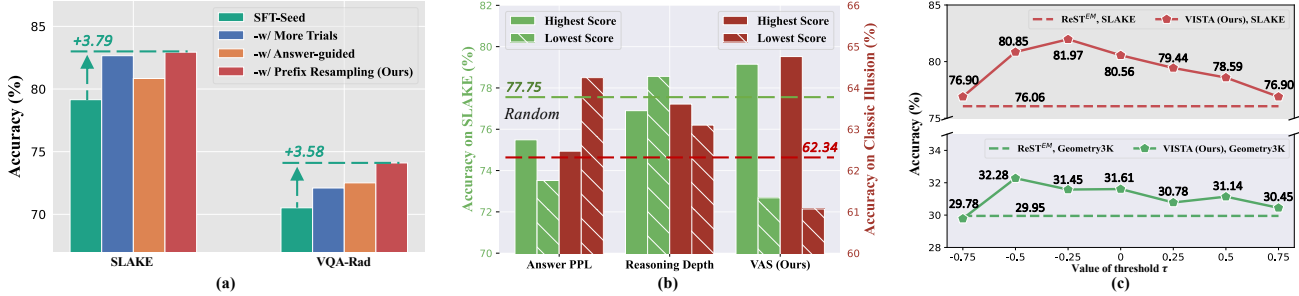


Figure 4. (a) Performance comparison of tuned Qwen2.5-VL-7B models using different data collection methods. (b) Performance comparison of tuned Qwen2.5-VL-3B models using different data selection metrics on SLAKE. (c) Parameter analysis of threshold  $\tau$  in VISTA on Qwen2.5-VL-3B models. Notably, in these experiments, we perform the self-improvement SFT training for one iteration.

in Table 4, from which we observe that: 1) Compared to SFT training, both DPO and GRPO training methods lead to much better performance, indicating the superiority of reinforcement learning in the reasoning MLLM field. 2) Our VISTA continues to surpass the baseline methods in both post-training paradigms, e.g., bringing +1.98% average gains against the powerful IRPO during DPO training.

### 4.3. More Analyses

**Impact of Prefix Resampling Strategy.** We first validate the effect of our *prefix resampling* strategy by comparing it with two representative baselines: 1) “-w/ More Trials” that allocates more trials to difficult queries (Tong et al., 2024); 2) “-w/ Answer-guided” that leverages the ground-truth answers to guide the reasoning (Ding et al., 2025). Notably, for a fair comparison, we ensure that the amount of sampled training data among all methods is comparable, and do not use the subsequent VAS method. The comparative results on Qwen2.5-VL-7B models are shown in Figure 4 (a). From these results, we can see that all methods consistently outperform the SFT-Seed baseline, confirming the importance of mitigating data imbalance. Among these methods, our prefix resampling strategy performs best in both reasoning tasks. We conjecture that the partially correct prefix contexts are more informative and reduce the difficulty of sampling more accurate solutions for challenging queries, thus alleviating the data imbalance problem effectively. More in-depth analyses of prefix resampling are shown in Appendix C.1.

**Impact of Vision-aware Attention Score.** In this part, we investigate the effect of our *vision-aware score* that aims to identify and filter out the undesired hallucinated solutions. For comparison, we use two representative counterparts as the baselines: 1) “Answer PPL” that employs the perplexity of solutions to quantify the model’s uncertainty during the reasoning (Cao et al., 2024), where solutions with smaller PPL are referred to better; 2) “Reasoning Depth” that leverages the JSD divergence between reasoning tokens’ hidden states at the final model layer and middle layer to quantify the reasoning depth (Chuang et al., 2023), where solutions with larger JSD scores are referred to better. In practice, after obtaining the self-generated candidate solutions via our prefix resampling strategy, we construct two self-training sets by selecting one solution for each query with the highest and lowest score across different metrics. Then, Qwen2.5-VL-3B-Instruct is fine-tuned on these two sets, respectively. In addition to the SLAKE task, all models are also evaluated on a sub-task of IllusionBench (Zhang et al., 2025), “Classic Illusion”, which is a cutting-edge multimodal hallucination detection benchmark. For reference, we also construct a training set by randomly selecting one correct solution for each query, and use it to fine-tune the model. The comparative results are illustrated in Figure 4 (b).

From the results on SLAKE, we can see that “Answer PPL” and “Reasoning Depth” metrics perform poorly in the self-improvement training of MLLMs, as they either cannot adequately meet the needs of model training (samples with high

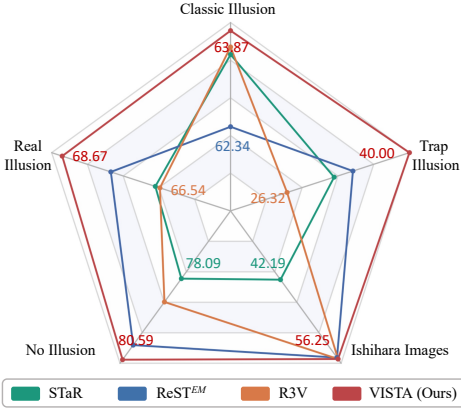


Figure 5. Performance comparison between different tuned Qwen2.5-VL-3B models on IllusionBench. Here, we perform the self-improvement SFT training on the VQA-Rad for one iteration.

scores perform worse) or even underperform the random baseline. Conversely, our vision-aware attention score can effectively reflect the quality of self-generated data, as training on solutions with the lowest scores leads to catastrophic performance degradation. This underscores the importance to alleviate the language prior bias problem, and to encourage the MLLMs to focus more on visual cues. This conclusion can also be proven by the results on the Classic Illusion set, as training on undesired solutions identified by our metric leads to more hallucinations. These results demonstrate the effectiveness of our metric. Additionally, we provide more analyses of our VAS metric in Appendix C.2.

**Parameter Analysis.** The threshold  $\tau$ , used to filter the undesired solutions, is an important hyperparameter in our VISTA framework. In this part, we analyze its effect by evaluating the VISTA performance with different  $\tau$  values, ranging from -0.75 to 0.75. The Qwen2.5-VL-3B-Instruct is used as the base model and evaluated on SLAKE and Geometry3K tasks. For reference, we compare our VISTA with the ReST<sup>EM</sup> baseline, and present the results in Figure 4 (c). As seen, compared to the baseline, VISTA with various  $\tau$  can achieve better performance, proving that VISTA is not very sensitive to the threshold. More specifically, too large  $\tau$  (e.g., 0.75) would lead to performance degradation, as many useful solutions might be filtered. Overall, in the case of  $\tau = -0.5$ , VISTA achieves the optimal performance, thus leaving it as our default setting in this work.

**Model Generalization.** Intuitively, by filtering the hallucinated training data, VISTA can achieve better model generalization. To verify it, we conduct experiments from two aspects: 1) hallucination alleviation and 2) out-of-distribution (OOD) evaluation. First, for 1), we test the models tuned with different self-improvement methods on the popular hallucination evaluation benchmark, IllusionBench (Zhang et al., 2025). The benchmark contains 5 categories, in-

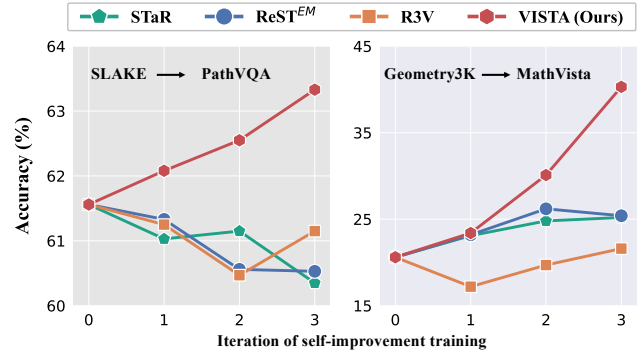


Figure 6. Comparison of OOD results between tuned Qwen2.5-VL-3B models using different self-improvement SFT methods. The x-axis denotes the index of self-improvement iteration.

cluding *Classic Illusion*, *Real Scene Illusion*, *No Illusion*, *Ishihara Images*, and *Trap Illusion*. In this experiment, we use the VQA-Rad as the training set, and illustrate the results of tuned Qwen2.5-VL-3B models on IllusionBench in Figure 5. Notably, all models are self-trained for one iteration. It can be seen that, while ReST<sup>EM</sup> performs well in the *No Illusion* category, it suffers from hallucinations in the other categories, indicating that self-training on the hallucination solutions could exacerbate model hallucinations. Conversely, by filtering these undesired solutions, our VISTA outperforms all the other counterparts and achieves the best performance across all hallucination categories.

Second, for 2), we evaluate the models trained on SLAKE on the OOD PathVQA (He et al., 2020) test set, while evaluating the models trained on Geometry3K on the MathVista (Lu et al., 2024) test set. The OOD results of different tuned Qwen2.5-VL-3B models are illustrated in Figure 6. We can observe that, in medical reasoning tasks, with the self-improvement iteration increasing, the tuned models using all baseline methods generally lead to worse OOD results. This phenomenon is similar to prior work (Wu et al., 2025). We conjecture that these models may suffer from overfitting due to imbalanced self-training data. Compared to these baselines, our VISTA methods consistently improve the OOD performance across all iterations. Similar to medical reasoning, on MathVista, VISTA also yields performance gains of up to +19.7% over the initial SFT model.

Moreover, to rigorously evaluate the OOD generalization of our method, we assess the tuned Qwen2.5-3B-VL models on several challenging benchmarks: MMMU (Yue et al., 2024), MathVerse (Zhang et al., 2024), and BLINK-Twice (JIANG et al., 2026). Specifically, for MMMU, we select 5 medicine-related subtasks as the test set. The OOD results after a single round of self-improvement SFT training with different methods are presented in Table 5. As shown, VISTA-SFT consistently outperforms all baselines across all OOD settings, demonstrating strong generalizability and validating

Table 5. More challenging OOD evaluation of Qwen2.5-3B-VL after single-round self-improvement SFT with different methods.

Method	SLAKE→		Geo3K→	
	MMMU	BLINK	MathVerse	BLINK
SFT-Seed	16.34	49.35	17.08	39.17
STaR	16.34	49.78	16.54	39.89
ReSTEM	14.04	47.62	15.52	37.95
R3V	14.78	44.73	12.34	37.81
<b>VISTA-SFT</b>	<b>17.64</b>	<b>51.23</b>	<b>21.76</b>	<b>40.26</b>

the ability of VAS to encourage genuine visual grounding. Overall, these results demonstrate that our VISTA can indeed improve the model generalization effectively.

☞ **Note:** Due to space limitations, we introduce the related works in Appendix A, more experimental details in Appendix B, and more experiments and analyses in Appendix C. Please refer to the Appendix for more details.

## 5. Conclusion

In this paper, we reveal that self-improvement training in MLLMs usually suffers from data imbalance and language prior bias problems. To this end, we propose VISTA that effectively harnesses self-improvement in MLLMs via two simple-yet-effective approaches: 1) *prefix resampling* and 2) *vision-aware attention score* (VAS). Specifically, prefix resampling first uses a trajectory recycling strategy to efficiently collect more accurate solutions for difficult queries, while VAS then leverages the internal attention information of MLLMs to quantify and filter the undesired solutions. Extensive experiments show that VISTA not only outperforms the other counterparts by a clear margin across various MLLMs and tasks, *e.g.*, bringing up to **+13.66%** average scores for Qwen2.5-VL-3B-Instruct model, but also improves the model generalization effectively.

## Impact Statement

For the ethics of our work, we take ethical considerations very seriously and strictly adhere to the ICML Ethics Policy. This paper proposes a new vision-aware self-improvement training framework to improve the multimodal reasoning performance of MLLMs. It aims to unleash MLLMs’ internal reasoning capabilities, rather than encouraging them to learn privacy knowledge that may cause an ethical problem. Moreover, all base models, training and evaluation datasets used in this paper are publicly available and have been widely adopted by researchers. Thus, we believe that this research will not pose ethical issues. For the potential societal consequences, we believe that there are many potential societal consequences of our work, but none of which we feel must be specifically highlighted here.

## Limitations

Our work has several potential limitations. First, our prefix resampling strategy retains the early correct prefix and regenerates the subsequent reasoning. While this effectively produces additional correct solutions for challenging queries, it may restrict trajectory diversity when the critical token appears late in the reasoning trajectory, causing the resampled solutions to share substantial overlap with the original. This could potentially lead to overfitting if such cases dominate the training data. Second, due to computational constraints, our experiments are conducted on relatively small-scale models (*e.g.*, 3B and 7B). Validating our VISTA method on larger-scale models (*e.g.*, 30B and 70B) or Mixture-of-Experts (MoE) architectures would further strengthen the credibility and generalizability of our approach, and we leave this exploration to future work.

## Acknowledgements

We are grateful to the anonymous reviewers and the area chair for their insightful comments and suggestions. This work was supported in part by the National Key Research and Development Program of China under Grant 2023YFC2705702, in part by the National Natural Science Foundation of China under Grant 62225113, U23B2048 and 625B2132, in part by the Innovative Research Group Project of Hubei Province under Grants 2024AFA017, in part by the Science and Technology Major Project of Hubei Province under Grants 2024BAB046 and 2025BCB026, and in part by the New Cornerstone Science Foundation through the XPLOER PRIZE. This work was also supported by WHU-Kingsoft Joint Lab. Dr Tao’s research is partially supported by NTU RSR and Start Up Grants. The numerical calculations in this paper have been done on the supercomputing system in the Supercomputing Center of Wuhan University.

## References

- Azaria, A. and Mitchell, T. The internal state of an llm knows when it’s lying. In *Findings of the Association for Computational Linguistics: EMNLP 2023*, 2023.
- Bai, S., Cai, Y., Chen, R., Chen, K., Chen, X., Cheng, Z., Deng, L., Ding, W., Gao, C., Ge, C., et al. Qwen3-vl technical report. *arXiv preprint arXiv:2511.21631*, 2025a.
- Bai, S., Chen, K., Liu, X., Wang, J., Ge, W., Song, S., Dang, K., Wang, P., Wang, S., Tang, J., et al. Qwen2.5-vl technical report. *arXiv preprint arXiv:2502.13923*, 2025b.
- Bai, Z., Wang, P., Xiao, T., He, T., Han, Z., Zhang, Z., and Shou, M. Z. Hallucination of multimodal large language

- models: A survey. *arXiv preprint arXiv:2404.18930*, 2024.
- Bertrand, Q., Bose, J., Duplessis, A., Jiralerspong, M., and Gidel, G. On the stability of iterative retraining of generative models on their own data. In *The Twelfth International Conference on Learning Representations*, 2024.
- Cao, Y., Kang, Y., Wang, C., and Sun, L. Instruction mining: Instruction data selection for tuning large language models. In *First Conference on Language Modeling*, 2024.
- Chen, J., Cai, Z., Ji, K., Wang, X., Liu, W., Wang, R., Hou, J., and Wang, B. Huatuogpt-o1, towards medical complex reasoning with llms. *arXiv preprint arXiv:2412.18925*, 2024.
- Cheng, K., YanTao, L., Xu, F., Zhang, J., Zhou, H., and Liu, Y. Vision-language models can self-improve reasoning via reflection. In *Proceedings of the 2025 Conference of the Nations of the Americas Chapter of the Association for Computational Linguistics: Human Language Technologies (Volume 1: Long Papers)*, 2025.
- Chuang, Y.-S., Xie, Y., Luo, H., Kim, Y., Glass, J. R., and He, P. Dola: Decoding by contrasting layers improves factuality in large language models. In *The Twelfth International Conference on Learning Representations*, 2023.
- Deng, S., Wang, K., Yang, T., Singh, H., and Tian, Y. Self-improvement in multimodal large language models: A survey. In *Findings of the Association for Computational Linguistics: EMNLP 2025*, 2025.
- Ding, Y., Xi, Z., He, W., Lizhuoyuan, L., Zhai, Y., Xiaowei, S., Cai, X., Gui, T., Zhang, Q., and Huang, X.-J. Mitigating tail narrowing in llm self-improvement via socratic-guided sampling. In *Proceedings of the 2025 Conference of the Nations of the Americas Chapter of the Association for Computational Linguistics: Human Language Technologies*, 2025.
- Feng, K., Gong, K., Li, B., Guo, Z., Wang, Y., Peng, T., Wu, J., Zhang, X., Wang, B., and Yue, X. Video-r1: Reinforcing video reasoning in mllms. In *Proceedings of the 39th International Conference on Neural Information Processing Systems*, 2025.
- Guan, X., Zhang, L. L., Liu, Y., Shang, N., Sun, Y., Zhu, Y., Yang, F., and Yang, M. rstar-math: Small llms can master math reasoning with self-evolved deep thinking. In *Forty-second International Conference on Machine Learning*, 2025.
- Gulcehre, C., Paine, T. L., Srinivasan, S., Konyushkova, K., Weerts, L., Sharma, A., Siddhant, A., Ahern, A., Wang, M., Gu, C., et al. Reinforced self-training (rest) for language modeling. *arXiv preprint arXiv:2308.08998*, 2023.
- Guo, D., Yang, D., Zhang, H., Song, J., Zhang, R., Xu, R., Zhu, Q., Ma, S., Wang, P., Bi, X., et al. Deepseek-r1: Incentivizing reasoning capability in llms via reinforcement learning. *arXiv preprint arXiv:2501.12948*, 2025.
- He, J., Zhu, K., Guo, H., Fang, J., Hua, Z., Jia, Y., Tang, M., Chua, T.-S., and Wang, J. Cracking the code of hallucination in llms with vision-aware head divergence. In *Proceedings of the 63rd Annual Meeting of the Association for Computational Linguistics (Volume 1: Long Papers)*, 2025.
- He, X., Zhang, Y., Mou, L., Xing, E., and Xie, P. Pathvqa: 30000+ questions for medical visual question answering. *arXiv preprint arXiv:2003.10286*, 2020.
- Hosseini, A., Yuan, X., Malkin, N., Courville, A., Sordani, A., and Agarwal, R. V-star: Training verifiers for self-taught reasoners. In *First Conference on Language Modeling*, 2024.
- Huang, A., Block, A., Foster, D. J., Rohatgi, D., Zhang, C., Simchowitz, M., Ash, J. T., and Krishnamurthy, A. Self-improvement in language models: The sharpening mechanism. In *The Thirteenth International Conference on Learning Representations*, 2025a.
- Huang, J., Gu, S., Hou, L., Wu, Y., Wang, X., Yu, H., and Han, J. Large language models can self-improve. In *Proceedings of the 2023 Conference on Empirical Methods in Natural Language Processing*, 2023.
- Huang, W., Liu, H., Guo, M., and Gong, N. Visual hallucinations of multi-modal large language models. In *Findings of the Association for Computational Linguistics: ACL 2024*, 2024.
- Huang, X., Wu, J., Liu, H., Tang, X., and Zhou, Y. Medvl-thinker: Simple baselines for multimodal medical reasoning. *arXiv preprint arXiv:2508.02669*, 2025b.
- Jaech, A., Kalai, A., Lerer, A., Richardson, A., El-Kishky, A., Low, A., Helyar, A., Madry, A., Beutel, A., Carney, A., et al. Openai o1 system card. *arXiv preprint arXiv:2412.16720*, 2024.
- Ji, K., Xu, J., Liang, T., Liu, Q., He, Z., Chen, X., Liu, X., Wang, Z., Chen, J., Wang, B., et al. The first few tokens are all you need: An efficient and effective unsupervised prefix fine-tuning method for reasoning models. *arXiv preprint arXiv:2503.02875*, 2025.
- JIANG, D., He, J., Zhou, B., Huang, Z., Yan, Z., Li, H., He, C., Li, W., et al. Blink-twice: You see, but do you observe? a reasoning benchmark on visual perception. *Advances in Neural Information Processing Systems*, 38, 2026.

- Jiang, Z., Chen, J., Zhu, B., Luo, T., Shen, Y., and Yang, X. Devils in middle layers of large vision-language models: Interpreting, detecting and mitigating object hallucinations via attention lens. In *Proceedings of the Computer Vision and Pattern Recognition Conference*, 2025.
- Koh, W., Oh, W., Jang, J., Lee, M., Kim, H., Kim, A. Y., Kim, J., Lee, J., Kim, T., and Yun, S.-Y. Adastar: Adaptive data sampling for training self-taught reasoners. In *Proceedings of the 39th International Conference on Neural Information Processing Systems*, 2025.
- Lau, J. J., Gayen, S., Ben Abacha, A., and Demner-Fushman, D. A dataset of clinically generated visual questions and answers about radiology images. *Scientific data*, 5(1), 2018.
- Leng, S., Zhang, H., Chen, G., Li, X., Lu, S., Miao, C., and Bing, L. Mitigating object hallucinations in large vision-language models through visual contrastive decoding. In *Proceedings of the IEEE/CVF Conference on Computer Vision and Pattern Recognition*, 2024.
- Lin, Z., Liang, T., Xu, J., Liu, Q., Wang, X., Luo, R., Shi, C., Li, S., Yang, Y., and Tu, Z. Critical tokens matter: Token-level contrastive estimation enhances llm’s reasoning capability. In *Forty-second International Conference on Machine Learning*, 2025.
- Liu, B., Zhan, L.-M., Xu, L., Ma, L., Yang, Y., and Wu, X.-M. Slake: A semantically-labeled knowledge-enhanced dataset for medical visual question answering. In *2021 IEEE 18th international symposium on biomedical imaging (ISBI)*, 2021.
- Liu, C., Xu, Z., Wei, Q., Wu, J., Zou, J., Wang, X. E., Zhou, Y., and Liu, S. More thinking, less seeing? assessing amplified hallucination in multimodal reasoning models. *arXiv preprint arXiv:2505.21523*, 2025a.
- Liu, N. F., Gardner, M., Belinkov, Y., Peters, M. E., and Smith, N. A. Linguistic knowledge and transferability of contextual representations. In *Proceedings of the 2019 Conference of the North American Chapter of the Association for Computational Linguistics: Human Language Technologies*, 2019.
- Liu, W., Zeng, W., He, K., Jiang, Y., and He, J. What makes good data for alignment? a comprehensive study of automatic data selection in instruction tuning. In *The Twelfth International Conference on Learning Representations*, 2024.
- Liu, W., Li, J., Zhang, X., Zhou, F., Cheng, Y., and He, J. Diving into self-evolving training for multimodal reasoning. In *Forty-second International Conference on Machine Learning*, 2025b.
- Lu, P., Gong, R., Jiang, S., Qiu, L., Huang, S., Liang, X., and Zhu, S.-c. Inter-gps: Interpretable geometry problem solving with formal language and symbolic reasoning. In *Proceedings of the 59th Annual Meeting of the Association for Computational Linguistics and the 11th International Joint Conference on Natural Language Processing (Volume 1: Long Papers)*, 2021.
- Lu, P., Mishra, S., Xia, T., Qiu, L., Chang, K.-W., Zhu, S.-C., Tafjord, O., Clark, P., and Kalyan, A. Learn to explain: multimodal reasoning via thought chains for science question answering. In *Proceedings of the 36th International Conference on Neural Information Processing Systems*, 2022.
- Lu, P., Bansal, H., Xia, T., Liu, J., Li, C., Hajjishirzi, H., Cheng, H., Chang, K.-W., Galley, M., and Gao, J. Mathvista: Evaluating mathematical reasoning of foundation models in visual contexts. In *The Twelfth International Conference on Learning Representations*, 2024.
- Masry, A., Do, X. L., Tan, J. Q., Joty, S., and Hoque, E. Chartqa: A benchmark for question answering about charts with visual and logical reasoning. In *Findings of the association for computational linguistics: ACL 2022*, 2022.
- Pang, R. Y., Yuan, W., Cho, K., He, H., Sukhbaatar, S., and Weston, J. Iterative reasoning preference optimization. In *Proceedings of the 38th International Conference on Neural Information Processing Systems*, 2024.
- Peng, X., Xia, C., Yang, X., Xiong, C., Wu, C.-S., and Xing, C. Regensis: LLMs can grow into reasoning generalists via self-improvement. In *The Thirteenth International Conference on Learning Representations*, 2025.
- Rafailov, R., Sharma, A., Mitchell, E., Ermon, S., Manning, C. D., and Finn, C. Direct preference optimization: your language model is secretly a reward model. In *Proceedings of the 37th International Conference on Neural Information Processing Systems*, 2023.
- Shao, Z., Wang, P., Zhu, Q., Xu, R., Song, J., Bi, X., Zhang, H., Zhang, M., Li, Y., Wu, Y., et al. Deepseekmath: Pushing the limits of mathematical reasoning in open language models. *arXiv preprint arXiv:2402.03300*, 2024.
- Singh, A., Co-Reyes, J. D., Agarwal, R., Anand, A., Patil, P., Garcia, X., Liu, P. J., Harrison, J., Lee, J., Xu, K., et al. Beyond human data: Scaling self-training for problem-solving with language models. *Transactions on Machine Learning Research*, 2023.
- Skean, O., Arefin, M. R., Zhao, D., Patel, N. N., Naghiyev, J., LeCun, Y., and Shwartz-Ziv, R. Layer by layer: Uncovering hidden representations in language models. In *Forty-*

- second International Conference on Machine Learning*, 2025.
- Song, Y., Zhang, H., Eisenach, C., Kakade, S. M., Foster, D., and Ghai, U. Mind the gap: Examining the self-improvement capabilities of large language models. In *The Thirteenth International Conference on Learning Representations*, 2025.
- Tong, Y., Zhang, X., Wang, R., Wu, R., and He, J. Dartmath: difficulty-aware rejection tuning for mathematical problem-solving. In *Proceedings of the 38th International Conference on Neural Information Processing Systems*, 2024.
- Wang, T., Li, S., and Lu, W. Self-training with direct preference optimization improves chain-of-thought reasoning. In *Proceedings of the 62nd Annual Meeting of the Association for Computational Linguistics*, 2024a.
- Wang, X., Wei, J., Schuurmans, D., Le, Q. V., Chi, E. H., Narang, S., Chowdhery, A., and Zhou, D. Self-consistency improves chain of thought reasoning in language models. In *International Conference on Learning Representations*, 2023.
- Wang, Y., Chen, W., Han, X., Lin, X., Zhao, H., Liu, Y., Zhai, B., Yuan, J., You, Q., and Yang, H. Exploring the reasoning abilities of multimodal large language models (mllms): A comprehensive survey on emerging trends in multimodal reasoning. *arXiv preprint arXiv:2401.06805*, 2024b.
- Wang, Y., Wu, S., Zhang, Y., Yan, S., Liu, Z., Luo, J., and Fei, H. Multimodal chain-of-thought reasoning: A comprehensive survey. *arXiv preprint arXiv:2503.12605*, 2025.
- Wen, X., Liu, Z., Zheng, S., Ye, S., Wu, Z., Wang, Y., Xu, Z., Liang, X., Li, J., Miao, Z., et al. Reinforcement learning with verifiable rewards implicitly incentivizes correct reasoning in base llms. *arXiv preprint arXiv:2506.14245*, 2025.
- Wu, T., Li, X., and Liu, P. Progress or regress? self-improvement reversal in post-training. In *The Thirteenth International Conference on Learning Representations*, 2025.
- Xu, W., Chan, H. P., Li, L., Aljunied, M., Yuan, R., Wang, J., Xiao, C., Chen, G., Liu, C., Li, Z., et al. Lingshu: A generalist foundation model for unified multimodal medical understanding and reasoning. *arXiv preprint arXiv:2506.07044*, 2025.
- Yang, C., Si, Q., Duan, Y., Zhu, Z., Zhu, C., Li, Q., Lin, Z., Cao, L., and Wang, W. Dynamic early exit in reasoning models. *arXiv preprint arXiv:2504.15895*, 2025a.
- Yang, S., Tong, Y., Niu, X., Neubig, G., and Yue, X. Demystifying long chain-of-thought reasoning. In *Forty-second International Conference on Machine Learning*, 2025b.
- Yuan, Z., Yuan, H., Li, C., Dong, G., Lu, K., Tan, C., Zhou, C., and Zhou, J. Scaling relationship on learning mathematical reasoning with large language models. *arXiv e-prints arXiv: 2308.01825*, 2023.
- Yue, X., Ni, Y., Zhang, K., Zheng, T., Liu, R., Zhang, G., Stevens, S., Jiang, D., Ren, W., Sun, Y., et al. Mmmu: A massive multi-discipline multimodal understanding and reasoning benchmark for expert agi. In *Proceedings of the IEEE/CVF conference on computer vision and pattern recognition*, 2024.
- Zelikman, E., Wu, Y., Mu, J., and Goodman, N. D. Star: self-taught reasoner bootstrapping reasoning with reasoning. In *Proceedings of the 36th International Conference on Neural Information Processing Systems*, 2022.
- Zhang, R., Jiang, D., Zhang, Y., Lin, H., Guo, Z., Qiu, P., Zhou, A., Lu, P., Chang, K.-W., Qiao, Y., et al. Mathverse: Does your multi-modal llm truly see the diagrams in visual math problems? In *European Conference on Computer Vision*. Springer, 2024.
- Zhang, Y., Zhang, Z., Wei, X., Liu, X., Zhai, G., and Min, X. Illusionbench: A large-scale and comprehensive benchmark for visual illusion understanding in vision-language models. *arXiv preprint arXiv:2501.00848*, 2025.
- Zheng, H., Xu, T., Sun, H., Pu, S., Chen, R., and Sun, L. Thinking before looking: Improving multimodal llm reasoning via mitigating visual hallucination. *arXiv preprint arXiv:2411.12591*, 2024.
- Zhong, Q., Ding, L., Cai, X., Liu, J., Du, B., and Tao, D. Kft: Knowledge-aware fine-tuning for boosting llms' domain-specific question-answering performance. In *Findings of the Association for Computational Linguistics: ACL 2025*, 2025.
- Zhong, Q., Ding, L., Liu, J., Du, B., Rutkowski, L., and Tao, D. Better, faster: Harnessing self-improvement in large reasoning models. *arXiv preprint*, 2026a.
- Zhong, Q., Wang, K., Xu, Z., Ding, L., Liu, J., and Du, B. Achieving > 97% on gsm8k: Deeply understanding the problems makes llms better solvers for math word problems. *Frontiers of Computer Science*, 2026b.
- Zhu, J., Wang, W., Chen, Z., Liu, Z., Ye, S., Gu, L., Tian, H., Duan, Y., Su, W., Shao, J., et al. Internvl3: Exploring advanced training and test-time recipes for open-source multimodal models. *arXiv preprint arXiv:2504.10479*, 2025.

## Appendix

**Roadmap.** In the part, we first introduce the related work in Appendix A, and then provide the experimental details in Appendix B. Lastly, we present more experiments and analyses in Appendix C.

### A. Related Work

**Post-training for Multimodal Reasoning.** Recently, we have witnessed the great success of long-CoT reasoning LLMs, *e.g.*, DeepSeek-R1 (Guo et al., 2025) and OpenAI o1 (Jaech et al., 2024), in a diversity of natural language processing tasks (Shao et al., 2024; Chen et al., 2024; Zhong et al., 2026b). Motivated by this, extending the advantage of long-CoT reasoning to multimodal context has attracted significant interest (Wang et al., 2024b; 2025; Zhu et al., 2025; Bai et al., 2025b;a). To achieve this goal, a common approach is to post-train the MLLMs with explicit reasoning trajectories (Huang et al., 2025b; Xu et al., 2025; Feng et al., 2025). However, such a method highly relies on extensive, high-quality reasoning trajectories, which are usually costly and time-consuming to obtain (Peng et al., 2025). While the new emerging Reinforcement Learning with Verifiable Rewards (RLVR) training paradigm (Guo et al., 2025; Wen et al., 2025) does not strictly require the explicit reasoning trajectories, cold-start training with these trajectories can effectively improve the performance and training efficiency (Yang et al., 2025b), which also underscores the importance of these trajectories.

**Self-improvement Training for MLLMs.** To reduce the reliance on explicit reasoning trajectories, a “self-improvement” training paradigm has been proposed, where models improve themselves using self-generated data without any external supervision. Prior works mainly focus on the self-improvement of LLMs (Zelikman et al., 2022; Yuan et al., 2023; Huang et al., 2023; Gulcehre et al., 2023; Wang et al., 2024a; Hosseini et al., 2024; Wu et al., 2025; Huang et al., 2025a; Song et al., 2025). For instance, in the SFT post-training setting, STaR (Zelikman et al., 2022) utilizes few-shot examples to gather self-synthesizing correct reasoning paths for SFT training, while RFT (Yuan et al., 2023) and ReST<sup>EM</sup> (Singh et al., 2023) extend STaR by sampling multiple responses for each question. In the preference learning setting, Pang et al. (2024) and Wang et al. (2024a) propose to construct preference pairs by using the self-generated correct responses as the pair winners and the incorrect responses as the pair losers. Recent advances attempt to extend self-improvement training to multimodal reasoning (Cheng et al., 2025; Liu et al., 2025b; Guan et al., 2025; Deng et al., 2025). Specifically, beyond ReST<sup>EM</sup>, Cheng et al. (2025) propose to construct the self-refine and self-select training data for better learning from mistakes.

Despite their effectiveness, we empirically find that these self-improvement methods usually suffer from data imbalance and language prior bias. Some prior studies also recognize these problems and attempt to address them by collecting more correct solutions for difficult queries (Tong et al., 2024; Ding et al., 2025; Koh et al., 2025) and designing metrics to measure the language priors (He et al., 2025; Liu et al., 2025a). However, these efforts either fail to exploit prior failed solutions fully or rely on external models and additional computational overhead to estimate the language prior bias. Different from them, we propose two simple-yet-effective approaches to address these problems efficiently. On the one hand, instead of solely allocating more trials to difficult queries, our *prefix resampling* strategy makes full use of the partial correct prefix context to achieve efficient data collection. On the other hand, although simple, our proposed *Vision-Aware Score* can accurately quantify the model’s attention to the visual context within seconds.

Notably, our work differs from the concurrent work (Zhong et al., 2026a) in three key aspects: 1) *Different research objectives.* The concurrent work focuses on self-improvement in LLMs and mainly addresses the overthinking issue, whereas we study self-improvement in MLLMs and target visual hallucinations specific to multimodal reasoning. 2) *Different methodologies.* Although both works involve alleviating data imbalance by reusing prior failed solutions, the concurrent work relies on ground-truth answers to verify intermediate reasoning steps, while our method does not require ground-truth supervision and instead leverages the model’s self-calibration to identify critical tokens. 3) *Different experimental settings.* The concurrent work evaluates on text-only tasks, whereas we conduct experiments on multimodal VQA tasks.

### B. More Experimental Details

#### B.1. Dataset Details

In this work, we conduct experiments on a diverse range of multimodal reasoning benchmarks. Here, we first provide some self-generated long-CoT examples in Figure 7, and then introduce the descriptions of these tasks as follows:

- **SLAKE:** SLAKE (Liu et al., 2021) is a widely-used medical visual question-answering (VQA) task, which contains both

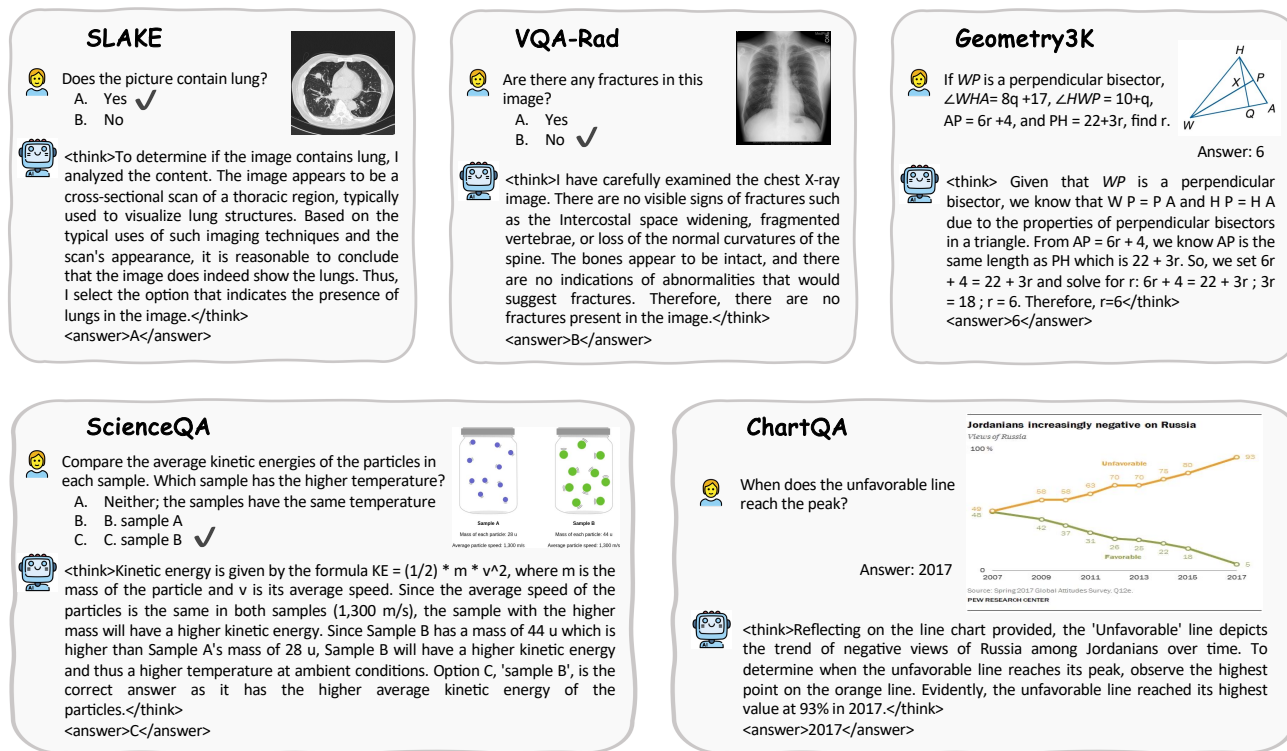


Figure 7. Examples of self-generated long-CoT data in various multimodal reasoning tasks.

bilingual closed-ended and open-ended questions across various modalities and human body parts. In this work, we only use the closed-ended English questions and their corresponding answers. By filtering the data, we finally obtain a training set with 1,681 samples, and a test set with 355 samples.

- **VQA-Rad**: VQA-Rad (Lau et al., 2018) is also a popular multimodal medical reasoning task, which contains 2,248 question-answer pairs and 315 radiology images. The dataset includes both open-ended questions and binary “yes/no” questions. Similar to SLAKE, we also use the closed-ended questions for model training and evaluation. Specifically, the final training and test sets have 940 and 251 samples, respectively.
- **Geometry3K**: Geometry3K (Lu et al., 2021) comprises 3,002 geometry problems. Here, to verify the effectiveness of our VISTA in more challenging tasks, we use a variant of Geometry3K<sup>3</sup> that converts the multiple-choice problems into open-ended ones. Specifically, there are 2,101 queries in the training set, and 601 queries in the test set.
- **ScienceQA**: ScienceQA (Lu et al., 2022) is a large-scale science QA task, which contains 21,208 multimodal multiple-choice questions from elementary and high school science curricula. Due to the limited computational resources, we use a subset of ScienceQA for model training and evaluation. Specifically, only the closed-ended questions with image context and grades higher than 6 are used in this work, resulting in 2,635 training samples and 813 test samples.
- **ChartQA**: ChartQA (Masry et al., 2022) is a large-scale chart reasoning benchmark covering 9.6K human-written questions and 23.1K generated questions. This benchmark evaluates MLLMs’ visual and logical reasoning capabilities. Similar to ScienceQA, we also sample a subset of ChartQA for a faster experimental validation. In particular, only the human-written questions with digit answers are selected, resulting in 3,233 training samples and 1,026 test samples.
- **PathVQA**: PathVQA (He et al., 2020) is a challenging medical VQA benchmark, containing a total of 5K pathology images and 32K question-answer pairs. We use the 3,362 closed-ended questions from the original test set to evaluate the OOD performance of models trained on SLAKE.

<sup>3</sup><https://huggingface.co/datasets/hiyouga/geometry3k>

- **MathVista:** MathVista (Lu et al., 2024) is a consolidated mathematical reasoning benchmark, which consists of three newly created datasets, 9 MathQA datasets, and 19 VQA datasets from the literature. In total, MathVista includes 6K examples collected from 31 different datasets. We use the 1,000 closed-ended test samples to evaluate the OOD performance of models trained on Geometry3K.
- **IllusionBench:** IllusionBench (Zhang et al., 2025) is a large-scale visual illusion benchmark, encompassing over 1K images, 5K question-answer pairs, and 1K golden text descriptions, covering the presence, causes, and content of illusions. Specifically, it contains five categories: 1) *Classic Cognitive Illusion*, including blur, distortion, paradox, and fictitious illusions—key examples of traditional synthetic illusions. 2) *Real Scene Illusion*, containing images that depict real-world objects and scenes, with unique and definite semantic descriptions. 3) *No Illusion*, depicting diverse subjects such as people, landscapes, and objects. 4) *Ishihara Images*, verified by vision-healthy individuals, where the patterns convey unique and definite semantics. 5) *Trap Illusion*, edited versions of classic visual illusions, resembling them in appearance but differing in physical properties.

Notably, for each task, the reasoning template is similar to that in DeepSeek-R1, *i.e.*, the reasoning process and answer are enclosed with `<think></think>` and `<answer></answer>` tags. Specifically, we use the following system prompt in our work:

#### System Prompt

A conversation between User and Assistant. The user asks a question, and the Assistant solves it. The assistant first thinks about the reasoning process in the mind and then provides the user a concise final answer in a short word or phrase. The reasoning process and answer are enclosed within `<think> </think>` and `<answer> </answer>` tags, respectively, *i.e.*, `<think> reasoning process here </think><answer> answer here </answer>`.

## B.2. Training and Evaluation Details

During the SFT training, we fine-tune each model with a batch size of 32 and a peak learning rate of  $1e-5$ . The total training epoch is set to 3. The max image pixels are set to  $512 \times 512$ . In the DPO training phase, the batch size is set to 16, and the peak learning rate is set to  $1e-5$ . All models are trained for 3 epochs. Both SFT and DPO training are performed using the popular LLaMA-Factory<sup>4</sup> toolkit, following prior work (Zhong et al., 2025). As for GRPO training, the batch size is set to 32, and the rollout size for each query is set to 10. The peak learning rate is set to  $1e-6$ . The maximum output length during on-policy sampling is set to 512. Each model is trained for 3 epochs. We use the EasyR1<sup>5</sup> as the training framework of GRPO. Notably, for the model optimizer of all settings, we keep the vision encoder and multimodal projector fixed, and only update the parameters of the LLM backbone. All experiments are conducted on 8 NVIDIA A800 (80GB) GPUs.

For the model evaluation, we use the greedy decoding method, *i.e.*, temperature set to 0 for reproducibility. The maximum output length is set to 2,048. All models are evaluated in a zero-shot manner. We extract the final answer enclosed within `<answer></answer>`. If no valid answer is extracted, the response is considered incorrect.

## C. More Experiments and Analyses

### C.1. Analysis of Prefix Resampling Strategy

**Effectiveness of prefix resampling.** To verify whether our *prefix resampling* can alleviate the data imbalance problem, we calculate the sampling success rate on the hardest queries, which did not obtain any correct solutions during the  $K$ -times self-generation processes. Figure 8 (a) illustrates the results of Qwen2.5-VL-3B-Instruct on several benchmarks, where the x-axis denotes the number of resampled correct solutions in a query, and the y-axis denotes the proportion of queries. As seen, although the vanilla data collection method struggles to sample any correct solutions for these difficult queries, our prefix resampling strategy can effectively improve the sampling success rate. Specifically, for both SLAKE and VQA-Rad tasks, more than 80% of these difficult queries can resample at least one correct solution, and nearly 40% of these queries have 4 or more correct solutions. While for the harder Geometry3K task, relatively fewer correct solutions are successfully resampled, our prefix resampling strategy still collects at least one correct solution for 37% difficult queries. To have a close look, taking the challenging Geometry3K task as an example, we further compare the correct solution distribution before

<sup>4</sup><https://github.com/hiyouga/LLaMA-Factory>

<sup>5</sup><https://github.com/hiyouga/EasyR1>

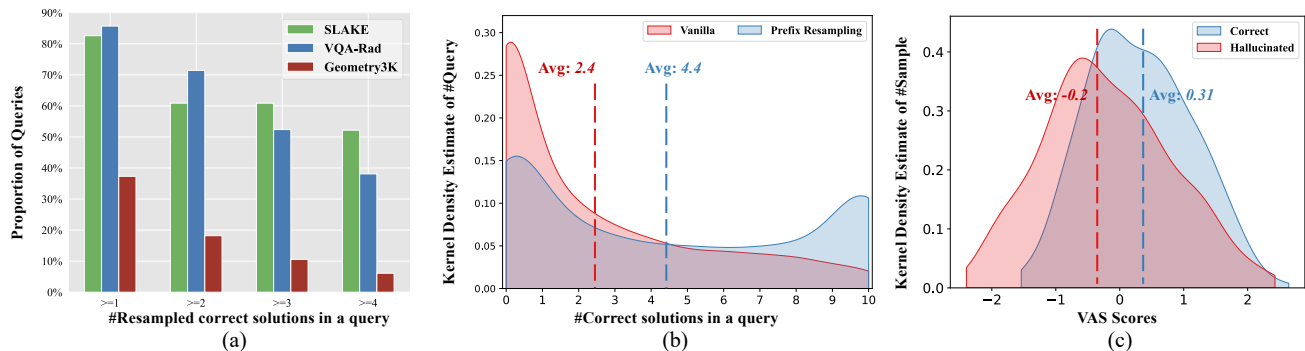


Figure 8. (a) Sampling success rate of our prefix resampling on the hardest queries (*i.e.*, without any prior correct solutions). The x-axis denotes the number of resampled correct solutions in a query. (b) Distribution of the number of correct tokens in a query before and after using our prefix resampling strategy. Here, we show the results on the challenging Geometry3K task. (c) Distribution of our VAS scores in correct and hallucinated solutions from the VQA-Rad task. Notably, Qwen2.5-VL-3B-Instruct is used in these experiments.

Table 6. **Perturbation strategy comparison.** Results on Qwen2.5-3B-VL after single-round self-improvement SFT training.

Method	SLAKE	VQA-Rad
ReST <sup>EM</sup>	76.06	69.72
<b>VISTA-Swap</b>	<b>80.85</b>	<b>74.10</b>
VISTA-Mask	78.31	70.12
VISTA-Noise	78.87	70.52

Table 7. **Effect of the Top- $k$  setting.** Results on Qwen2.5-3B-VL after single-round self-improvement SFT training.

Top- $k$	SLAKE	VQA-Rad
1	80.28	72.91
<b>5</b>	<b>80.85</b>	<b>74.10</b>
10	80.00	71.71
50	78.03	69.72

and after using the prefix resampling strategy. As illustrated in Figure 8 (b), with the help of prefix resampling, we can collect more correct solutions for difficult queries, *i.e.*, improving the average number of correct solutions per query from 2.4 to 4.4. These results demonstrate that our prefix resampling indeed alleviates the data imbalance effectively.

**Effectiveness of the token position swap mechanism.** To obtain the rewritten solution, we perform a swap operation on the original negative solution. A natural question is whether this swap strategy is effective and why alternative perturbation strategies, such as masking or noise injection, are not adopted instead. We clarify that the swap operation leverages the model’s internal self-calibration in response to context changes, rather than introducing random perturbations. Specifically, by swapping the visual and instruction token order, the context structure is altered, exposing model uncertainty about the critical token (Lin et al., 2025). In contrast, masking and noise injection may corrupt valid content and cause significant semantic shifts, thereby impairing the model’s precision in locating critical tokens. To further validate the effectiveness of the swap method, we replace it with masking and noise injection in VISTA and conduct experiments on Qwen2.5-3B-VL. The comparative results under single-round self-improvement SFT training are presented in Table 6. As shown, the swap method achieves superior performance compared to both masking and noise injection. Additionally, it is worth noting that although masking and noise injection perform slightly worse, they still outperform the baseline ReST<sup>EM</sup>, suggesting that VISTA exhibits a reasonable degree of robustness to noise in critical token detection.

**Effect of the Top- $k$  setting.** During prefix resampling, we use the Top-5 token predictions to detect critical tokens. Here, we investigate the effect of the top- $k$  setting by varying  $k \in \{1, 5, 10, 50\}$  and comparing the resulting performance of VISTA. The comparative results on Qwen2.5-3B-VL are presented in Table 7. We observe that when  $k$  is too small ( $k=1$ ), the model suffers from over-calibration, truncating at very early prefix tokens and degrading sampling efficiency. Conversely, when  $k$  is too large ( $k=50$ ), the model overlooks many critical tokens, reducing the effectiveness of prefix resampling. With  $k=5$ , the model achieves the best overall performance, and we therefore adopt it as our default setting.

## C.2. Analysis of VAS Metric

**Reliability of VAS.** By analyzing the quality of self-generated candidate solutions, we found that some solutions suffer from visual hallucinations (Huang et al., 2024; Bai et al., 2024; Zheng et al., 2024), even though they produce the correct answers. As shown in examples of Figure 9, during the reasoning process, MLLMs may describe some things that do not exist in the image (denoted as “Description Hallucination”), or exhibit a conflict between the reasoning chain and its final

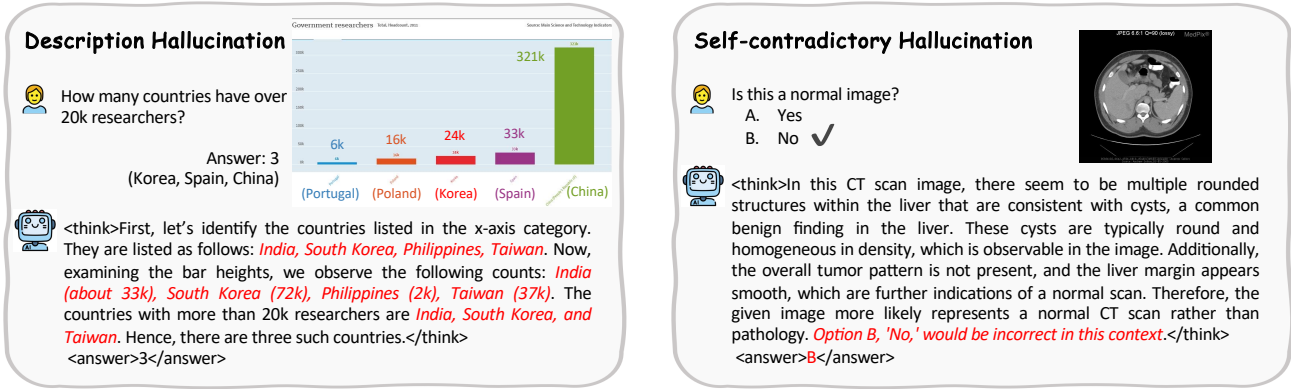


Figure 9. Examples of two types of self-generated hallucinated solutions, where the hallucinated contents are highlighted in red.

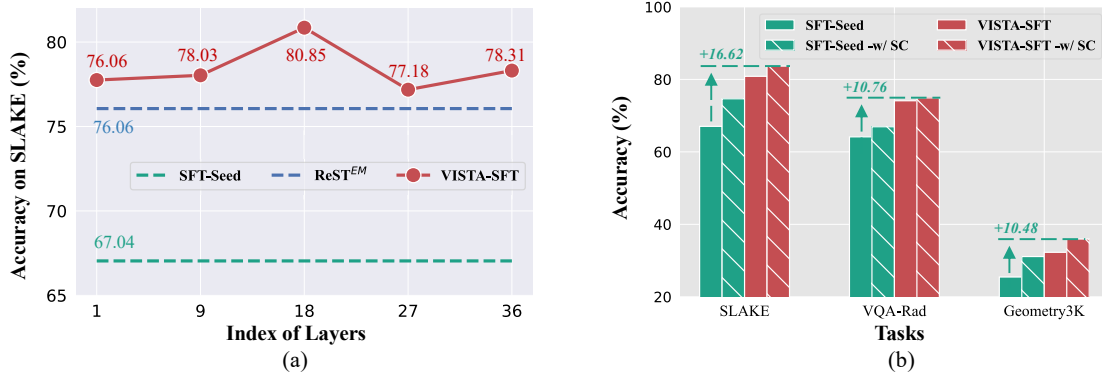


Figure 10. (a) Analysis of layer depth for calculating VAS scores. (b) Performance comparison between with and without the self-consistency method. Notably, we report the results of Qwen2.5-VL-3B-Instruct models self-trained for one iteration.

answer (denoted as “Self-contradictory Hallucination”). We speculate that the main reason for this problem may lie in MLLMs’ strong language priors, which affect the focus and usage of visual cues. To this end, we propose a vision-aware attention score (VAS) to quantify it. Here, to verify whether our metric can identify the hallucinated solutions, we first prompt the GPT-4o to determine whether the candidate solution is hallucinated. In practice, we randomly sample 500 queries from the training set of VQA-Rad, which are then used to collect the candidate solutions by Qwen2.5-VL-3B-Instruct. For each self-generated candidate solution of these queries, we enforce GPT-4o to detect whether there are any non-existent contents in the reasoning traces or whether the reasoning chain conflicts with the final answer. By doing so, we finally collected 586 hallucinated solutions. Correspondingly, 586 non-hallucinated solutions are randomly selected for comparison. For these paired data, we calculate their VAS scores and illustrate the distribution in Figure 8 (c). Obviously, the hallucinated solutions have a lower VAS score than the correct ones. Specifically, the average VAS score of hallucinated solutions is -0.2, while the average VAS score of correct solutions is 0.31. That is, our VAS score can effectively distinguish between hallucinated solutions and correct ones, proving its reliability.

**Impact of layer depth for calculating VAS scores.** As mentioned in §3, we use the attention output of the middle layer of MLLMs to calculate the VAS scores. Here, we investigate the impact of different layer depths by comparing the performance of tuned Qwen2.5-VL-3B models using different VISTA configurations on SLAKE. Specifically, for the Qwen2.5-VL-3B-Instruct containing 36 layers, we vary the layer used for calculating VAS scores across {1, 9, 18, 27, 36} and illustrate the comparative results in Figure 10 (a). For reference, we also include the results of SFT-Seed and ReST<sup>EM</sup> methods. All models are self-improved for one iteration. As seen, VISTA with varied layer depth can consistently outperform the other baseline methods, indicating that VISTA is relatively robust to the choice of layer. Moreover, when using the middle layer (i.e., 18-th layer), VISTA achieves the best performance. We conjecture that the middle layer encodes richer and more useful semantic information (Skean et al., 2025; Azaria & Mitchell, 2023; Liu et al., 2019), and plays a crucial role in processing visual information (Jiang et al., 2025), thus resulting in more accurate VAS scores. Based on these observations, we choose to adopt the middle layer of  $\mathcal{M}_{t-1}$  for calculating VAS scores in this work.

### C.3. Comparison and Compatibility with Inference-time Method

Since the goal of our work is to propose a self-improvement training, rather than to optimize inference, we do not compare our VISTA with inference-time methods, such as Self-Consistency (SC) (Wang et al., 2023), in the main experiments. Nevertheless, considering that SC is widely used to enhance models’ reasoning performance, we include it in this experiment. Specifically, for the implementation of SC, we sample five solutions for each test query and select the majority-vote answer as the final prediction. Figure 10 (b) presents the comparative results of tuned Qwen2.5-VL-3B models on several benchmarks, where “-w/ SC” means using the SC method. As seen, by increasing the test-time compute, SC indeed improves the multimodal reasoning performance of SFT-Seed models effectively. However, it still underperforms our zero-shot VISTA method. More encouragingly, combining the VISTA and SC methods consistently yields further performance improvements. For instance, in the SLAKE task, VISTA equipped with SC achieves a +16.62% performance gain over the SFT-Seed model. These results prove the compatibility of our VISTA with the inference-time SC method.

### C.4. Efficiency of VISTA

A potential concern regarding our VISTA framework is its efficiency, as it requires additional forward passes of MLLMs. We acknowledge that VISTA introduces some computational overhead during data collection. However, it is worth noting that VISTA simultaneously reduces the training data volume, thereby improving training efficiency. Taking Qwen2.5-3B-VL on SLAKE as an example, we report the wall-clock time (in minutes) of different self-improvement SFT methods in Table 8. As shown, the total cost of VISTA is comparable to that of ReST<sup>EM</sup> and significantly lower than that of R3V, while achieving substantially better performance. We therefore consider the additional inference overhead to be a worthwhile trade-off given the consistent performance gains.

Table 8. Wall-clock time comparison (in minutes) of different self-improvement SFT methods on SLAKE using Qwen2.5-3B-VL.

Method	Data Collection	Training	Total
STaR	1.3	2.5	3.9
ReST <sup>EM</sup>	2.3	26.2	28.6
R3V	3.3	49.7	53.0
<b>VISTA-SFT</b>	12.0	17.2	29.2

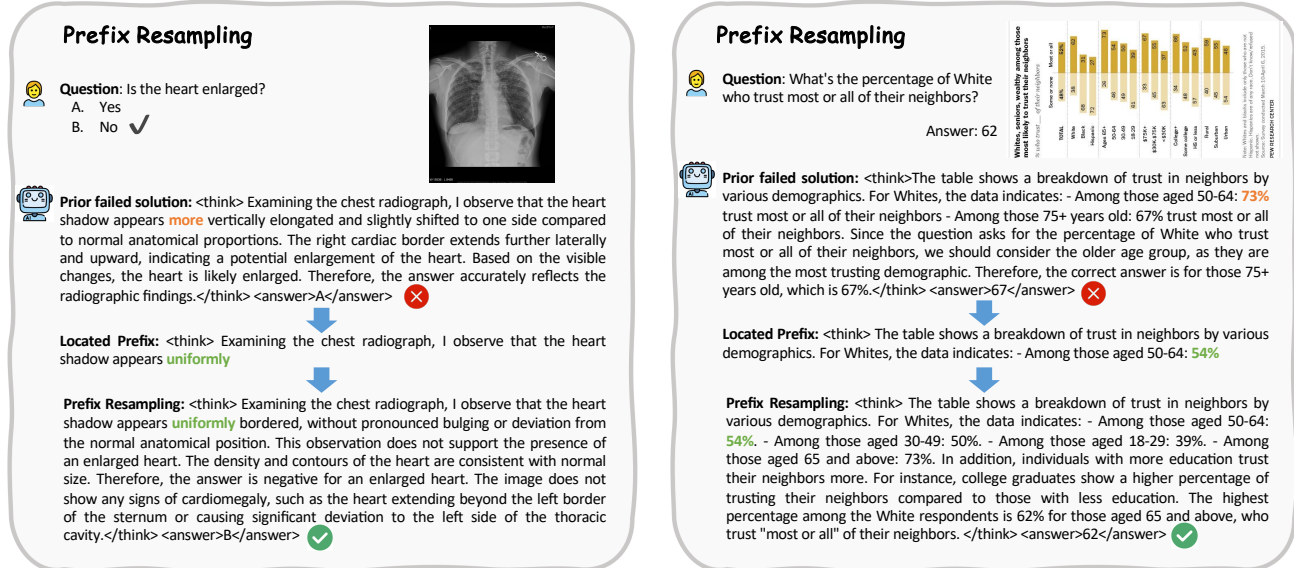


Figure 11. Illustration of our prefix resampling strategy. Notably, we use examples from the SLAKE (Left) and ChartQA (Right).

### C.5. Case Study

To better understand our methods and demonstrate their effectiveness, we provide some cases in this part. First, Figure 11 shows the comparison of self-generated solutions between before and after using our prefix sampling strategy. We present the self-generated results of Qwen2.5-VL-3B-Instruct on the SLAKE and ChartQA tasks. As seen, our prefix sampling can accurately locate the critical tokens and salvage valid initial reasoning from failed attempts by continuing sampling from the

correct prefix contexts. Figure 12 shows the comparison of VAS scores between correct and hallucinated candidate solutions in the VQA-Rad and ChartQA tasks. Moreover, we also compare the test results of models trained using different methods and illustrate the comparison in Figure 13. Obviously, with the help of VISTA, Qwen2.5-VL-3B models can produce more reliable reasoning traces and make more accurate predictions. These qualitative analyses also prove VISTA’s effectiveness.

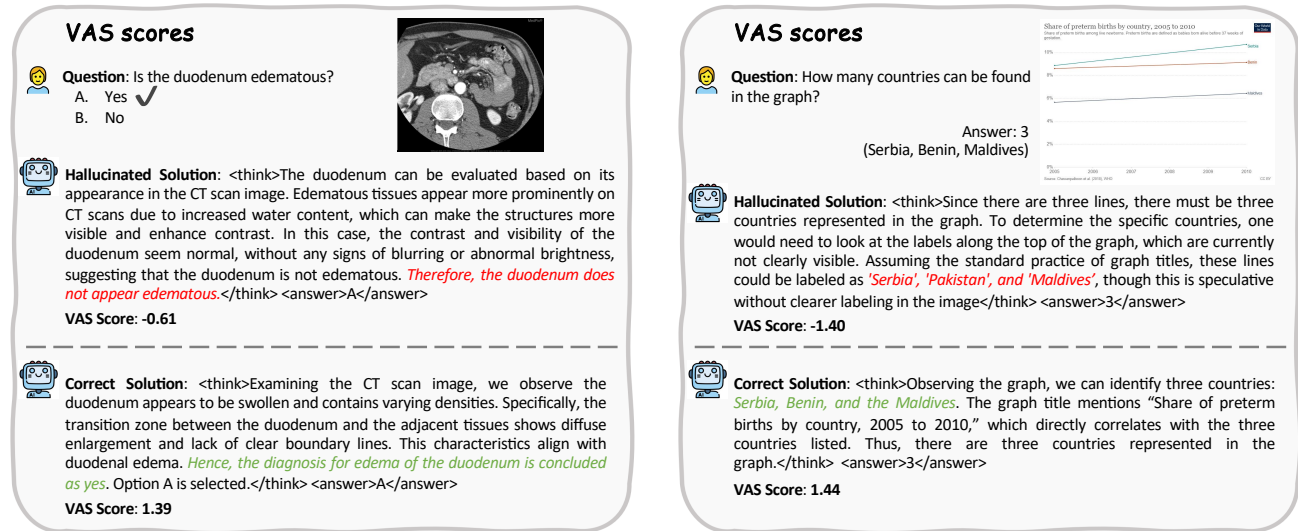


Figure 12. Examples of self-generated solutions with our VAS scores in the VQA-Rad (Left) and ChartQA (Right) tasks.

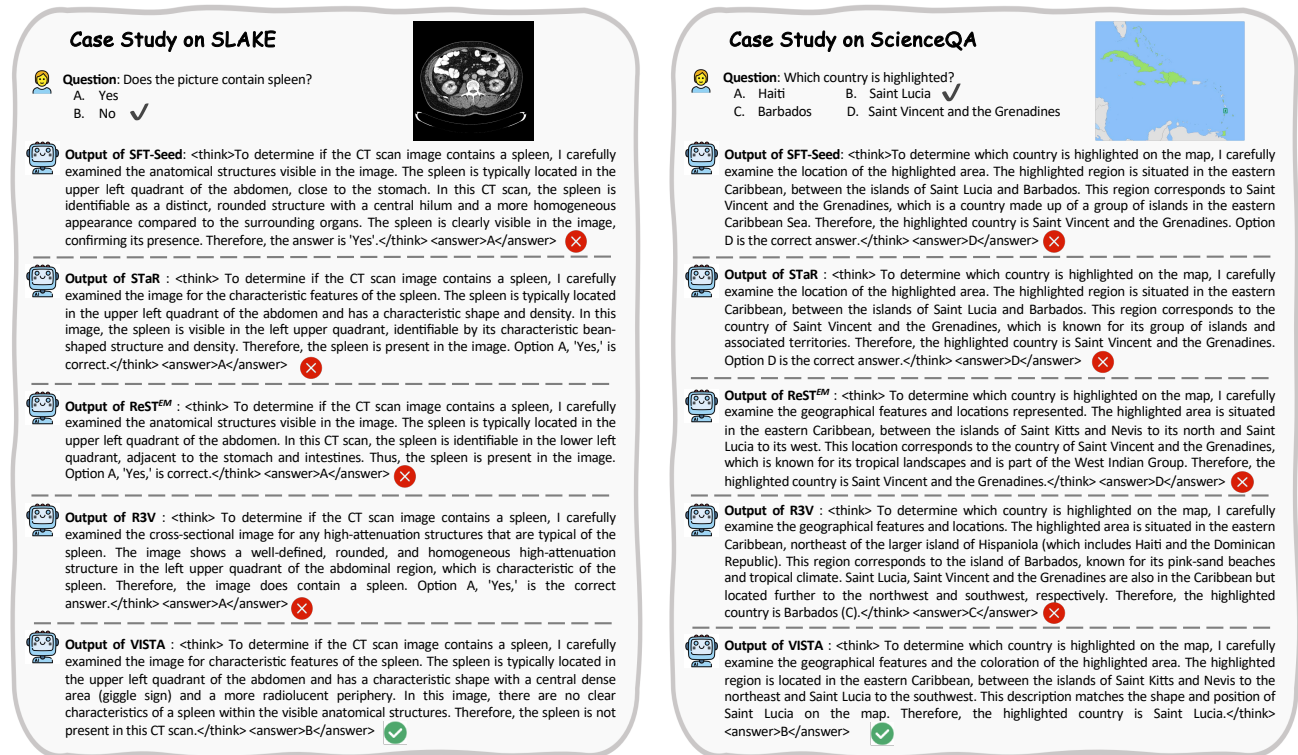


Figure 13. Examples of solutions predicted by Qwen2.5-VL-3B models tuned with different self-improvement training methods.

---

**Algorithm 1** Self-improvement Training with VISTA

---

```

1: Input: base model  $\mathcal{M}_{base}$ , training dataset  $\mathcal{D} = \{(x_i, y_i)\}$ , where  $x_i = \{x_i^{sys}, x_i^{vis}, x_i^{ins}\}$ 
2: Output: self-improved model  $\mathcal{M}_T$ 
3: Obtain a seed reasoning dataset by prompting  $\mathcal{M}_{base}$  to generate correct solutions for  $\mathcal{D}$  via some few-shot examples
4: Fine-tune  $\mathcal{M}_{base}$  on the seed dataset to get initial reasoning model  $\mathcal{M}_0$ 
5: for  $t \in [1, T]$  do
6:   # Data Collection
7:   Obtain  $K$  candidate solutions  $\{(r_i^k, \hat{y}_i^k)\}_{k=1}^K$  generated by  $\mathcal{M}_{t-1}$  for each  $x_i \in \mathcal{D}$ 
8:   Verify the correctness of candidate solutions, and split them into two sets:
     positive set  $\mathcal{D}_t^p = \{(x_i, r_i^{k_p}, \hat{y}_i^{k_p}) \mid x_i \in \mathcal{D}; k_p \in [1, K]; \mathbb{I}(\hat{y}_i^{k_p}, y_i) = 1\}$ 
     negative set  $\mathcal{D}_t^n = \{(x_i, r_i^{k_n}, \hat{y}_i^{k_n}) \mid x_i \in \mathcal{D}; k_n \in [1, K]; \mathbb{I}(\hat{y}_i^{k_n}, y_i) = 0\}$ 
9:
10:  # Prefix Resampling
11:  for Each sample  $(x_i, r_i^{k_n}, \hat{y}_i^{k_n}) \in \mathcal{D}_t^n$  do
12:    Swap the order of visual tokens, e.g., from “ $x_i^{vis} + x_i^{ins}$ ” to “ $x_i^{ins} + x_i^{vis}$ ”
13:    Feed the paraphrased sample into  $\mathcal{M}_{t-1}$  to obtain the Top-5 token predictions for each token  $o_n$  in  $r_i^{k_n}$ 
14:    for Each token  $o_n \in r_i^{k_n}$  do
15:      if  $o_n \notin \text{Top}_5(o_{n-1})$  then
16:        Replace the  $o_n$  with the new Top-1 predicted token  $o'_n = \text{Top}_1(o_{n-1})$  and truncate the subsequent reasoning steps
17:        Concatenate the original query with the truncated reasoning traces as a prefix
18:        Break
19:      else
20:        Continue
21:      end if
22:    end for
23:    Feed the prefix context into  $\mathcal{M}_{t-1}$  to resample  $J$  solutions and add the correct solutions into  $\mathcal{D}_t^p$ 
24:  end for
25:
26:  # Vision-aware Attention Score
27:  for Each query  $x_i \in \mathcal{D}_t^p$  do
28:    Calculate the VAS score  $\mathbf{VAS}_i^k$  for each correct solution  $(r_i^{k_p}, \hat{y}_i^{k_p})$  as Eq. 4
29:    Update the dataset  $\mathcal{D}_t^p$  by filtering out the undesired solution with  $\mathbf{VAS}_i^k < \tau$ 
30:  end for
31:
32:  # SFT Training
33:  Fine-tune  $\mathcal{M}_{base}$  with  $\mathcal{L}_{\text{SFT}}$  in Eq. 1 on the  $\mathcal{D}_t^p$ 
34:  # or DPO Training
35:  Obtain a pairwise dataset  $\mathcal{D}_t^{\text{pairs}} = \{(x_i, r_i^{k_p}, \hat{y}_i^{k_p}, r_i^{k_n}, \hat{y}_i^{k_n}) \mid k_p, k_n \in [1, K]\}$ , where  $(r_i^{k_p}, \hat{y}_i^{k_p}) \sim \mathcal{D}_t^p$  and  $(r_i^{k_n}, \hat{y}_i^{k_n}) \sim \mathcal{D}_t^n$ 
36:  Train  $\mathcal{M}_{base}$  with  $\mathcal{L}_{\text{DPO+NLL}}$  in Eq. 2 on  $\mathcal{D}_t^{\text{pairs}}$ 
37: end for

```

---